Applied Energy 303 (2021) 117603

Contents lists available at ScienceDirect

Applied Energy

journal homepage: www.elsevier.com/locate/apenergy

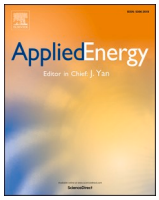

Application of upscaling methods for fluid flow and mass transport in multi-scale heterogeneous media: A critical review

Xiaoying Zhang [a], Funing Ma [a], Shangxian Yin [b], Corey D Wallace [c], Mohamad Reza Soltanian [c,d], Zhenxue Dai [a,e,*], Robert W. Ritzi [f], Ziqi Ma [a], Chuanjun Zhan [a], Xiaoshu Lü [g]

[a] College of Construction Engineering, Jilin University, Changchun 130026, China
[b] North China Institute of Science & Technology, Langfang 065201, China
[c] Department of Geology, University of Cincinnati, Cincinnati, OH, USA
[d] Departments of Environmental Engineering, University of Cincinnati, Cincinnati, OH, USA
[e] Engineering Research Center of Geothermal Resources Development Technology and Equipment, Ministry of Education, Jilin University, Changchun, China
[f] Earth and Environmental Sciences Department, Wright State University, Dayton, OH, USA
[g] Department of Electrical Engineering and Energy Technology, University of Vaasa, P.O.Box 700, FIN-65101 Vaasa, Finland

HIGHLIGHTS

- The scale dependency of fluid flow and reactive solute transport parameters was discussed across scales.
- A clear guideline was provided for selecting appropriate upscaling methods for practical applications.
- Functions, assumptions, and limitations of deterministic and stochastic upscaling methods were addressed comparatively.
- Critical insights into the scaling issues were prospected for modeling fluid flow in multi-scale subsurface systems.

ARTICLE INFO

Keywords:
Upscaling
Fluid flow
Reactive transport
Multi-scale heterogeneous media
Geological statistics

ABSTRACT

Physical and biogeochemical heterogeneity dramatically impacts fluid flow and reactive solute transport behaviors in geological formations across scales. From micro pores to regional reservoirs, upscaling has been proven to be a valid approach to estimate large-scale parameters by using data measured at small scales. Upscaling has considerable practical importance in oil and gas production, energy storage, carbon geologic sequestration, contamination remediation, and nuclear waste disposal. This review covers, in a comprehensive manner, the upscaling approaches available in the literature and their applications on various processes, such as advection, dispersion, matrix diffusion, sorption, and chemical reactions. We enclose newly developed approaches and distinguish two main categories of upscaling methodologies, deterministic and stochastic. Volume averaging, one of the deterministic methods, has the advantage of upscaling different kinds of parameters and wide applications by requiring only a few assumptions with improved formulations. Stochastic analytical methods have been extensively developed but have limited impacts in practice due to their requirement for global statistical assumptions. With rapid improvements in computing power, numerical solutions have become more popular for upscaling. In order to tackle complex fluid flow and transport problems, the working principles and limitations of these methods are emphasized. Still, a large gap exists between the approach algorithms and real-world applications. To bridge the gap, an integrated upscaling framework is needed to incorporate in the current upscaling algorithms, uncertainty quantification techniques, data sciences, and artificial intelligence to acquire laboratory and field-scale measurements and validate the upscaled models and parameters with multi-scale observations in future geo-energy research.

* Corresponding author at: College of Construction Engineering, Jilin University, Changchun 130026, China.
E-mail address: dzx@jlu.edu.cn (Z. Dai).

https://doi.org/10.1016/j.apenergy.2021.117603
Received 19 April 2021; Received in revised form 8 August 2021; Accepted 10 August 2021
Available online 20 August 2021

1. Introduction

Subsurface geological formations exhibit heterogeneous physical and chemical properties generated from dynamic geological [1], geochemical processes [2], and human activities [3] such as oil–gas-rock interactions. Heterogeneity is ubiquitous across all scales ranging from intra-granular pores and soil aggregatesto local and entire geological formations as shown in Fig. 1 [4]. At different scales, the major components of formation heterogeneity consist of physical and chemical properties such as the pore geometry [5], pore and grain size [6], mineral composition [7], sediment layering [8], lithology [9], and fracture distribution [10]. How to handle the pervasive heterogeneity in large-scale natural geological media is one of the major barriers to a comprehensive understanding of fluid flow and mass transport to the majority of hydrogeologists [11]. Neglecting heterogeneity properties may thus cause biased estimations of the model parameters and structures and considerable uncertainty of prediction results [12].

Mathematical modeling is often the most important and efficient simulation method for fluid flow, solute transport, and other subsurface water–oil-gas interaction processes [13–15]. Accuracy in the estimation of model parameters may increase the reliability of model predictions [16], but in the presence of heterogeneity and associated preferential flow paths, physical flow and transport parameters, as well as geochemical reaction rates, are found to differ by orders of magnitude with increasing time or distance, often referred to as the "*scale effect*" [17]. As an illustration, it is a common mistake to predict contaminant or solute migration at a large-scale field site using dispersivity measured at a fine scale in the laboratory, but finding the actual dispersion range in the field is much larger than the predictions [18]. Ignoring the scale effect of transport parameters results in erroneous projections of mass transport, such as spreading rates or arrival times, leading to severe consequences for health risk assessments [19], extreme event predictions [20], and reactive mixing features [21].

If using high-resolution computational grids to compensate the field spatial variability [22], the computational costs are exceptionally high in solving millions of diverse, discretized equations over thousands of time steps [23]. The cost is even heavier in the context of sensitivity studies, inverse modeling, or Monte Carlo analyses, which require running the computer code multiple times [24]. Therefore, it is of fundamental and practical importance to accurately predict flow and transport behaviors at large scales based on an understanding of parameter variations at smaller scales with affordable computational costs [25]. The use of suitable methods in tackling this problem is referred to as "*upscaling*". *It is the process of replacing a heterogeneous domain with a homogeneous one, such that both produce the same response when acted upon by the same boundary conditions* [26]. This process is illustrated in Fig. 2. The parameters in the fine model are often called "local" or "cell" parameters, while those in the coarse model are called "block" parameters.

The upscaling issue covers a broad range of topics in different study areas, from academic studies to industry applications [27]. Generally speaking, upscaling has diverse practical applications in energy industries that involved numerical modeling of fluid flow and mass transport in porous media or geological formations, for example, the prediction of cumulative oil and gas production [28], design of enhanced oil recovery schemes in operation [29], safety assessment in nuclear waste disposal [30], flow behavior of supercritical carbon dioxide and its reactive transport with minerals in carbon dioxide sequestration [31], evaluation of hydrocarbons migration in oil shale reservoirs [32]. Upscaling investigations and applications are increasingly common in the last 30 years, and the number of upscaling-related publications has increased exponentially, as shown in Fig. 3.

According to Bierkens and Gaast [33], pore and continuum scales are often identified by different governing equations (Fig. 1). In pore-scale simulations, the Navier-Stokes/Boltzmann equations are solved directly or approximately in the pore spaces to obtain flow fields [34]. Correspondingly, the fluid flow on a continuous scale can be described with semi-empirical models, such as Darcy's law. Therefore, the continuum scale is also called Darcy's scale, and it may be divided into three spatial scales: laboratory, field-site, and regional scales [35]. The laboratory-scale includes regular flow cell, batch, column, and sandbox experiments from millimeters to meters. The field-site scale often refers to a formation domain where the site well tests or field tracer tests are conducted. On a regional scale, it indicates entire or major parts of aquifers with horizontal scales of the order of tens of kilometers, much larger than the formation thickness (tens to hundreds of meters), which can be characterized by geophysical data. Upscaling refers to the translation from a small scale to a larger one, for instance, from the pore scale (micro to millimeter) to the continuum scale, or from laboratory scale (centimeters) to the subsequent passage to the field and regional scale (kilometers).

Following the establishment of the upscaling concept in porous

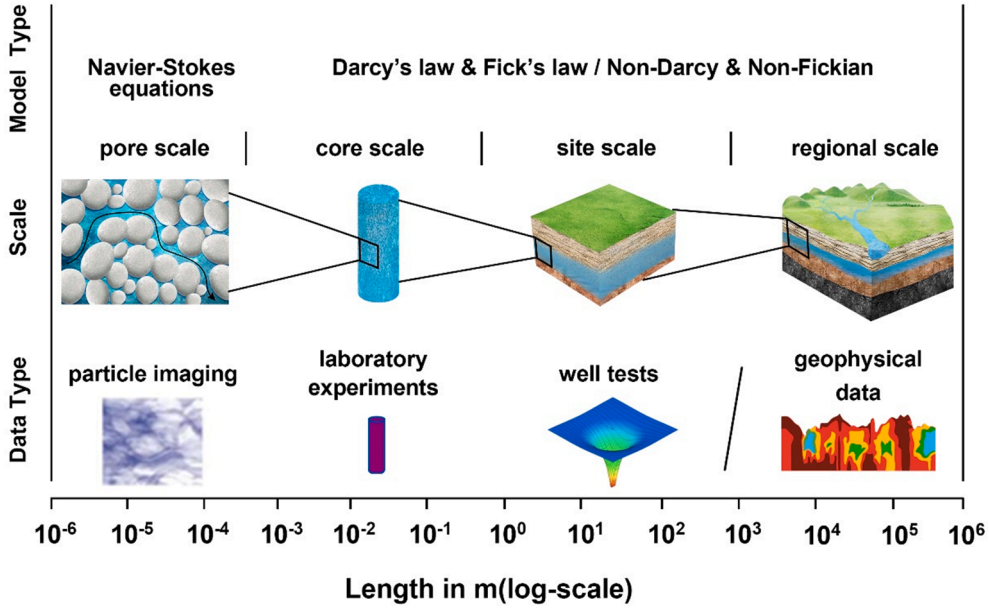

Fig. 1. Illustration of the model and measurement type variations at different scales with different measures. The fluid flow in the micro pore scale is often mapped by imaging approach and represented with N-S equation. The flow in the macro scale is primarily described with Darcy's law and Fick's law. Under some circumstances where Darcy's Law or Fick's Law do not fit, the alternate non-Darcy or non-Fickian expressions may be selected but as well established with an "averaged/homogenization" concept. The survey in the field scale mostly relys on the geophysical investigation or distributed monitoring wells. Note that the classification is not absolute, the methods can be utilized alternatively or coupled together in specific conditions.

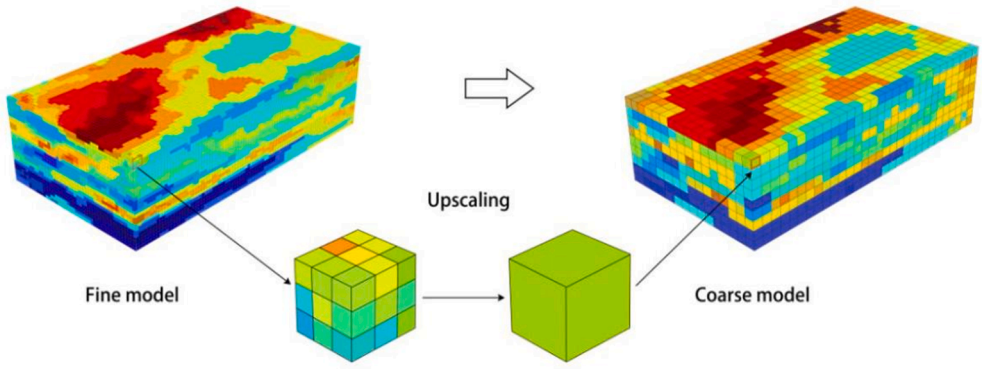

Fig. 2. Conceptual model of upscaling "local" parameters on a fine scale to "block" parameters on a coarse scale. Upscaling is a mathematical methodology to estimate physical and chemical parameters/properties of geophysical models at larger scales from an understanding of the measurement of parameter values at smaller scales [24].

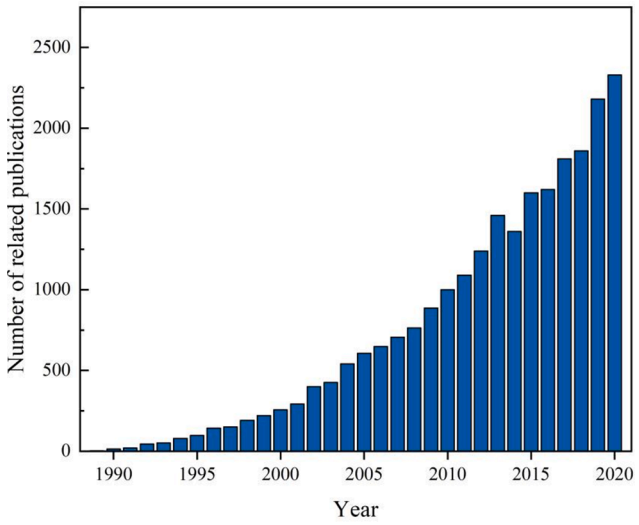

Fig. 3. Quantity of papers on the topic of upscaling during 1990–2020 from the web of science index; the number of published articles increased exponentially in the past 30 years.

media, many theoretical and computational methods have been developed [36]. Early efforts by Cushman [37] and Neuman [38] mainly used deterministic concepts to build large-scale hydraulic conductivity around assumed homogeneity within geological units. Sufficient data from site investigations are needed and the fine-scale information is then projected onto coarser-scale blocks of equal or unequal sizes explicitly. With technological developments for characterizing heterogeneity, a stochastic theory is developed by assuming heterogeneous property distributions as stationary, correlated, and random processes. The spatial probability distribution statistics of the block parameters are acquired from the statistical features of the smaller-scale parameters, which are assumed to compose a random field. It permits a coherent allocation of values at points where measurements have not been taken based on the values detected at measurement points. As a result, the stochastic approaches usually require available site-specific geological measurements to formulate statistical structures, and thus are not valid for media with a large spatial covariance. In the next step, concepts that visualize heterogeneity as nonstationary stochastic processes which have stationary increments (stochastic fractals and random walk) are considered. Recently, fractal theory, percolation theory, wavelet analysis, and artificial intelligence are gradually adopted in subsurface upscaling applications [39]. Furthermore, with the increase in model complexity involving biological and water–rock interactions, upscaling has also been extended to diffusion and sorption parameters representing biogeochemical properties in both porous and fractured media [40,41].

To understand the diverse upscaling approaches, many issues have been raised correspondingly. What are the functions, requirements, or limitations of the upscaling methods? How can reactive transport parameters, especially geochemical parameters, be upscaled? Are there successful modern approaches and techniques? All these issues have not been clearly addressed in previous studies. As a result, there are no clear guidelines yet on how to select appropriate methods when dealing with practical applications. Therefore, a comprehensive review that discusses the fundamental principles, applications, and limitations of these upscaling approaches is critical for providing a better understanding of upscaling concepts and approaches that have been developed over the past few decades, as well as its implications and future directions. The goal of this article is to integrate contemporary insights into the scaling issues associated with fluid flow and mass transport. In Section 2, we present the governing equations at the Darcy scale to analyze both fundamental physical processes and chemical reactions, discuss which parameters have scaling effects, and present the mechanisms involved. After establishing this framework, the primary upscaling approaches are separately presented with their mathematical formulations and practical applications. Section 3 demonstrates direct methods for upscaling hydraulic conductivity or permeability. Section 4 emphasizes the methods that can be applied to dispersivity and reactive parameters besides conductivity. Section 5 presents the principles and limitations of widely used stochastic methods. Section 6 discusses the issues associated with current upscaling algorithms, how to select appropriate implementation methods, and provides more useful insights into future work and challenges.

2. Dynamics of water flow and solute transport and scale dependency of parameters

2.1. Governing equation

In porous media, the most extensively used governing equation for mass transport is the advection–dispersion equation (ADE). By assuming that net solute movement is represented by the combination of an advective component and a random diffusive component, the conventional ADE derives the spatial and temporal solute concentration using the form [42]:

$$R\frac{\partial C}{\partial t} = \frac{\partial}{\partial x_i}\left(D_{ij}\frac{\partial C}{\partial x_j} - u_i C\right) + rC \tag{2.1}$$

where C denotes the concentration of the solute, u_i denotes velocity in direction i, x_i is the spatial coordinate in direction i, and t is time. D_{ij}

denotes the hydrodynamic dispersion coefficient. R is the retardation factor and often accounts for adsorption and desorption. rC represents the gain or loss contributions from reactions with a reaction rate of r. The ADE is defined as the divergence of a vector field. Given a vector field (**J**) and a unit normal vector (**n**), the divergence represents the proportion of total flux across a closed surface (S) to a unit volume (V) within the surface when the volume is reduced to zero.

$$\nabla\cdot\mathbf{J} \equiv \lim_{\mathrm{V}\to 0}\frac{1}{\mathrm{V}}\iint_{\mathrm{S}}\mathbf{J}\cdot\mathbf{n}\mathrm{dS} \tag{2.2}$$

The limit of the integral implies that the vector function **J** is smooth as V tends to zero. For solute transport, **J** represents solute flux, and thus the solute flux through a surface into a unit volume results in a specified value when the given volume is reduced. The solute is therefore assumed to travel through an equivalent porous medium with connected pore spaces or a network of connected fractures. The fluid is assumed to be incompressible and to have negligible viscosity under the assumption of Gaussian mixing. Variation in the solute flux is generally caused by either the impacts of mean velocity (i.e., advection) or velocity deviations (i.e., dispersion). Reducing the selected volume in Eq. (2.2) causes the velocity variations to vanish and the dispersive flux is reduced to zero [43]. Therefore, if we could obtain the detailed velocity distribution at a fine enough scale, the advective transport would theoretically duplicate reality without considering dispersion. As the access to the complex macroscopic subsurface is limited, constituting one of the reasons for introducing dispersive transport to adjust and correct such calculations.

The transportation of solutes with the bulk movement of a fluid can be described by the flow continuity equation and Darcy's equation [45]:

$$\nabla\bullet(\rho\mathbf{u}) + \mathrm{w} = -\frac{\partial(\mathrm{n}\rho)}{\partial \mathrm{t}} \tag{2.3}$$

$$\mathbf{u} = -\frac{\mathbf{K}}{n}\nabla h \tag{2.4}$$

where **u** represents the impact of micro-scale variability in the velocity field, **K** denotes the hydraulic conductivity tensor, n is the porosity of the porous medium, h is the hydraulic head, and w is the external sources and sinks. In the following sections, K is designated instead of **K** for a homogeneous fluid at the scale of V. The random movement of dispersion as dispersion coefficient tensor **D** can be expressed by two mechanisms:

$$\mathbf{D} = \alpha\mathbf{u} + \mathbf{D}^{*} \tag{2.5}$$

where α is dispersivity, and **D*** is the result of molecular diffusion due to concentration differences. The dispersivity is artificially separated into two components: a longitudinal component in the mean flow direction, and a transverse component in the orthogonal direction. The longitudinal dispersivity (α_L) controls the movement of the forefront of the solute plume, while the transverse dispersivity (α_T) governs the transverse spreading of the plume.

2.2. Scale dependency of hydraulic conductivity

From Eq. (2.3), the groundwater velocity field directly depends on K. Experiments with varying sediment and rock types have investigated the scale dependency of K with measurements in different scales. Generally, scale-related disparities in K for homogeneous media, such as quartz arenites or fine sand, are narrowly distributed and can be ignored [44]. The scale effect of K is mainly evidenced in varied heterogeneous media, including unconsolidated sediments, crystalline rocks, and fractured media [45]. The larger the scale of the experiment, or targeting volume, the higher the K it corresponds [46]. Consistent with these results, Neuman [38] indicated that "*porous and fractured media appear to follow the same idealized scaling rule for both flow and transport, raising a question about the validity of many distinctions commonly drawn between such media.*"

Most prior studies on the scale effect of K compare small-scale laboratory tests (i.e., permeameter tests) with medium- (i.e., slug tests) or large-scale (i.e., pumping tests) aquifer tests [47]. Though in some studies, the measurement scale is taken as the distance of the radius of influence, the measurement scale of K behavior is better expressed as the volume of the affected geological unit [48]. We collected the measured conductivity data from different sites in a variety of geologic media (Fig. 4). Generally, K slightly increases with increasing test radius when the characterized volume is larger than 1 m^3 but has a wide-spreading range on a constant scale. For example, at a specified spatial scale (e.g., the field scale on the order of 10^2-10^3 m), K may vary by several orders of magnitude across multiple measurement scales (e.g., from 1 m^3 to 10^3 m or larger). At the micro-scale, no clear shift of K is observed with volume variation. Factors that influence the scale effect of K include the scale of investigation, the data acquisition technique, and the geological formation investigated [44]. Often, the quality of K estimates differs based on the limitations of the measurement technology, and the values are not usually validated even though the scale effect can be mainly dependent on it. Although Fig. 4 shows that the conductivity measurements increase with scale, it is worth noting that large-scale measurements are usually used for sampling sedimentary facies assemblages with more coarse-grain facies, while small-scale (volume $< 10^{-3}$ m^3) measurements sample mainly individual facies with more fine-grain facies. Then, the small-scale measurements may neither include samples from the same facies as in the larger-scale samples that were measured nor include them in the correct proportions. Therefore, the left part (volume $< 10^{-3}$ m^3) with more noises may be ignored from the scaling analysis of the hydraulic conductivity.

2.3. Scale dependency of transport parameters

2.3.1. Dispersivity

Scale-dependent solute dispersion in saturated media is a well-known phenomenon that has been studied extensively using experimental and numerical methods [53]. Dispersivity is not only dependent on physical factors, such as grain size and aquifer spatial scales, but also the variation of chemical interactions between the solution and the sediment [54]. The study of longitudinal dispersivity is more in-depth than transverse dispersivity. A series of laboratory and field tests conducted on a scale ranging from 0.3 m to 8 m revealed that α_L varied linearly with the mean travel distance from 0.035 cm to 50 cm [55]. Abgaze and Sharma [56] investigated dispersivity as scale increased

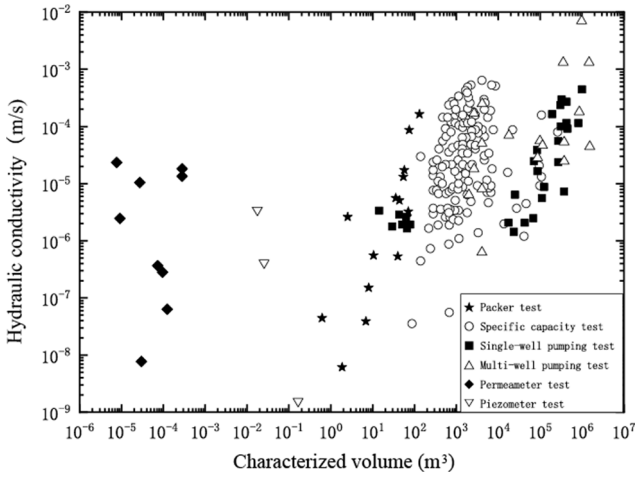

Fig. 4. The hydraulic conductivity variation with increasing scale as expressed in volume from varied measurement techniques based on data in [49–52]. Different symbols represent the results from different test types.

from 0.75 km up to 100 km; the field data typically ranged between 0.01 m and 5500 m. Values in fractured and karst media appear to spread over a similar range [57]. Conversely, little transverse dispersivities were observed in other field experimental data, suggesting that there is a limited transverse spreading of contaminant plumes. Plots of dispersivity coefficients in porous and fractured media from previous studies show that longitudinal dispersivity tends to increase with scale (Fig. 5), typically ranging over 2–3 orders of magnitude. The number of collected data for α_T is smaller than for α_L, but its overall trend is similar to α_L (Fig. 6).

From the traditional view, solute concentration is strongly correlated with the velocity field in the advective-dispersion model, likely related to the wide array of velocity distributions induced by subsurface heterogeneity. Velocity is not equal at every point in flow space. At the microscopic scale, velocity is maximum along the centerline of each pore and is zero on the pore walls. The centerline velocity, as well as the spread of the velocity, differs across pores of varying sizes. At the same time, flow direction changes as the fluid traverses the convoluted paths of the pore structure. As the solutes travel farther, the spreading sphere increases, encountering increasing scales of heterogeneity. Increased variations in the velocity fields, therefore, lead to a broader distribution of travel times and a larger dispersivity. The introduction of a new arbitrary volume in Eq. (2.2) alters the first derivative of surface flux, and inaccuracies in porosity measurements produce errors in solute plume transport velocity measurements [58]. This is the main reason for discrepancies in dispersivities and the necessity to introduce scaled parameters to compensate for the ill-defined divergence in a continuously varied medium when using an ADE in the field. Thus, to some extent, the dispersion scale effect depends on the capacity of models to characterize the velocity field in porous media. If the models accurately quantify the velocity field distribution driven by heterogeneity, the scale effect may be negligible [59].

2.3.2. Diffusion coefficient

Molecular diffusion is used to describe the irregular thermal motion of molecules. It is often ignored in large-scale solute transport where advection and dispersion are considered, but field studies have shown that, in low-flow systems, diffusion can be a significant transport process [62]. For instance, in natural or engineered barriers for waste disposal sites (i.e., compacted clays), molecular diffusion becomes the predominant process in the transport of aqueous species [63]. The coefficient of molecular diffusion typically depends on the solute, but for common anions and cations, it generally varies between 10^{-10} and 10^{-11} $m^2\ s^{-1}$.

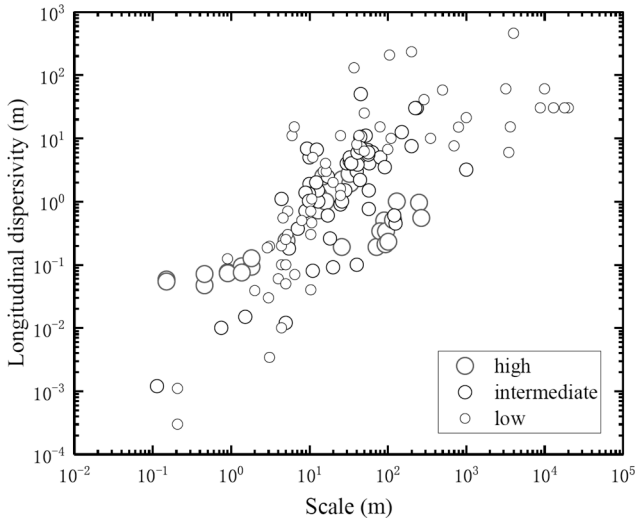

Fig. 5. Distribution of longitudinal dispersivity α_L across scales. The data is mainly collected from [60] and [61]. The circle sizes represent the data reliability. The detailed information about the reliability criteria can be referred to [60].

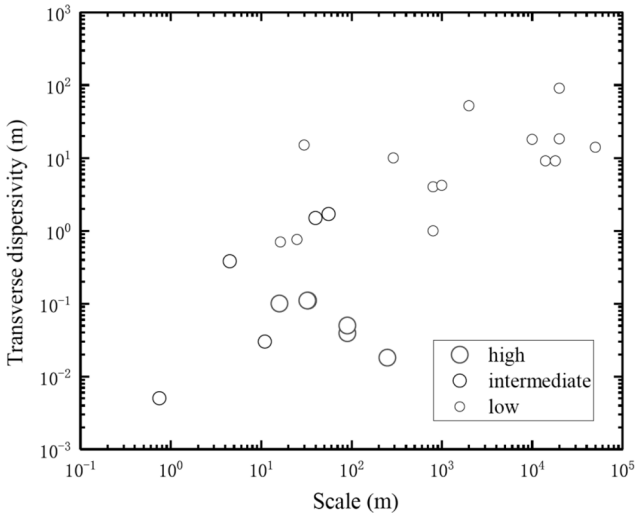

Fig. 6. Distribution of transverse dispersivity α_T across scales. The data is mainly collected from [60] and [61]. The circle sizes represent the data reliability. The detailed information about the reliability criteria can be referred to [60].

For Fickian flow, the molar flux from diffusion is proportional to the gradient of concentration. The diffusion flux, N_i, can be expressed as

$$N_i = -D_i^* \nabla C_i \tag{2.6}$$

where for a given species i, N_i represents the molar flux (mol $m^{-2}\ s^{-1}$), D_i is the molecular diffusion coefficient ($m^2\ s^{-1}$), and C_i is the solute concentration (mol m^{-3}). For dilute solutions with constant D_i, Fick's second law is directly derived from the mass continuity equation.

$$\frac{\partial C_i}{\partial t} = D_i^* \nabla^2 C_i \tag{2.7}$$

In practice, the matrix diffusion coefficient D_m is often used to represent diffusion in a matrix, which is expressed as D_i in free water multiplied by matrix tortuosity. In fractured systems and karst aquifers, D_m is recognized as the main reason for the retarded transport of solute, which results from the retained solute within the matrix structure [64]. The effective mass transfer coefficient (C_{MT}) is calculated to describe a given solute exchange rate between fractures and the rock matrix material in modeling. It is related to the effective fracture aperture (b), the effective matrix porosity (φ), and the effective diffusion coefficient (D_m) [65].

$$C_{MT} = \frac{\widetilde{\varphi}\sqrt{\widetilde{D}_m}}{b} \tag{2.8}$$

The effective diffusion coefficient is often higher at the field scale (kilometer) than at laboratory scales and tends to increase with the testing scales [66]. In crystalline rock, D_m is at least three orders of magnitude higher at the kilometer scale than that measured in the laboratory.

The need for an upscaled effective diffusion coefficient in such media is twofold: not only does diffusion spread solute through the slow-moving water, but preferential flow pathways created by the fracture network create a relatively large contact surface for water and solute to diffuse into the rock matrix [67]. Unfortunately, the magnitude and extent of small-scale fractures, which may greatly increase the area of the fracture-matrix interface, are barely represented in numerical models, which likely explains that the effective diffusion coefficients calculated from field data are relatively large [68]. Further, the relatively large matrix porosity near the fracture-matrix interface has been

shown to enhance the effective matrix diffusion coefficient [69] and may be the product of complex fractures characterized by a thin fracture zone with several interconnected sub-fractures. The effective diffusion tensor for non-linear reactions with large rates relative to diffusion is a function of the reaction rate [70].

2.3.3. Sorption parameters

As contaminants are transported in groundwater through an aquifer, their rate of movement may be less than the average flow rate of the groundwater. Sorption is a key process to slow down the contaminant migration in an aquifer. In this context, sorption refers to the removal of solute from the aqueous phase to a solid phase, as in a classical sorption isotherm batch experiment [71]. The process includes both adsorption, where the solute clings to an exterior solid surface, and absorption, where the solute clings to interior surfaces by diffusing into the porous solid. The measurement of a sorption isotherm until equilibrium is observed is used to quantify sorption. The partition coefficient, K_d, is one parameter that is used to describe the equilibrium ratio after a given reaction time between the amount of contaminant adsorbed per mass of the solid phase to the amount remaining in solution per solution volume. The measurement of K_d corresponds to a given ion under a specified experimental condition in a specified material and thus varies when the environmental conditions change. Consequently, the extrapolation of K_d obtained from a particular experimental setting to other adsorbents, adsorbates, or aqueous conditions like electrolyte concentrations and pH is infeasible [72].

Sorption can be described using any of the various forms of isotherms that have been proposed. The linear isotherm, which follows the same principle as Henry's Law, is the simplest and is defined as $S = K_d C$ [73]. C is the concentration remaining in the solution (ML^{-3}) and S is the weight of the contaminant sorbed by the solid. K_d in the linear isotherm is the sorption coefficient (L^3M), and here it is equivalent to the distribution coefficient. In contrast, the sorption isotherm of some organic or inorganic contaminants exhibits nonlinear sorption, such as cadmium and trace elements desorption [74]. Other isotherms, including the Freundlich, Langmuir, and two-sites sorption isotherms, are introduced to describe such sorption properties [75]. In these cases, the sorption coefficient is not equal to the distribution coefficient. For example, in the Freundlich isotherm, $S = K_f C^n$ (K_f is termed the Freundlich coefficient), K_d is equivalent to $K_f C^{n-1}$. Though in some previous studies, the sorption isotherm concept overlaps with the distribution coefficient or partition coefficient, here, such terms are clarified to avoid confusing the reader.

In practice, the retardation factor R is preferred in place of K_d to describe the delays associated with sorption/desorption [54]. Here, R is expressed as $R = 1 + \rho_b/nK_d$, where ρ_b and n are the bulk density and the porosity of the medium, respectively. In ADE equations, directly multiplying R by the time-variant solute concentration better represents the solute transport at the field sites with low-permeability layers or zones (e.g., sandy aquifers or fractured rock) [76]. The sorption parameters described above (K_d and R) are also scale-dependent and have been addressed as reactive solutes in sediments [77]. The estimated effective retardation factors may either increase or decrease with distance [78] and are influenced by several factors, including: how the test hydraulic gradient is generated (natural or forced); how the parameters $\ln(K)$ and $\ln(K_d)$ are correlated (absence of correlation or negative correlated); how mean arrival times are determined; and what the calculation method used is (i.e., spatial moments, temporal moments). Field-scale retardation factors also exhibit time-dependency, even with simple linear equilibrium sorption [79], but such dependency is not the focus of discussion in this review.

Sorption as well influences the migration and behavior of radionuclides in the subsurface. The scale dependency of uranium sorption/desorption is crucial in the risk assessment of nuclide-contaminated sites and geological repository systems for un-reprocessed, spent nuclear fuel. The adsorption partition coefficients of uranium have been observed to fluctuate over several orders of magnitude between pH 7 and pH 9 in different minerals [80]. In-situ tracer experiments conducted at the Äspö Hard Rock Laboratory indicate that the radionuclide retention properties of fractured crystalline bedrock are three to four orders of magnitudes higher in the laboratory.

2.4. Scale dependency of reaction rates

2.4.1. Mineral reaction rates

Mineral dissolution and precipitation is a crucial process in many earth and environmental processes, including rock and soil geochemical weathering [81]; global CO_2 fixation and geological sequestration [8]; migration of heavy metals and radionuclides to the biosphere [82]; biogeochemical cycles [83]; and the release, transport, and remediation of mineral-bound contaminants [84]. As one of the most important and rapid mineral reactions in the subsurface [85], calcite dissolution is used as an example to illustrate the scale dependency of the reaction rate for a specific kinetic mineral reaction. Though the form of rate laws may vary for different mineral reactions, considering potential factors involved in the reaction rate calculations, the associated principles for calcite can be extrapolated to other mineral phases [86]. Three parallel reaction schemes are involved in the dissolution [87]:

$$CaCO_3(s) + H^+ \rightleftharpoons Ca^{2+} + HCO_3^-$$

$$CaCO_3(s) + H_2CO_3^* \rightleftharpoons Ca^{2+} + 2HCO_3^-$$

$$CaCO_3(s) \rightleftharpoons Ca^{2+} + CO_3^{2-}$$

In the reaction, H^+ is consumed, thereby releasing Ca^{2+} to the aqueous solution. The Transition State Theory can be used to describe the calcite dissolution rate [87]:

$$r_{CaCO_3} = \left(k_1 a_{H^+} + k_2 a_{H_2CO_3^*} + k_3\right)\left(1 - \frac{IAP}{K_{eq}}\right) \tag{2.9}$$

where r_{CaCO3} (mol m^{-2} s^{-1}) is the microscopic calcite reaction rate (normalized to mineral surface area); k_1, k_2, and k_3 (mol m^{-2} s^{-1}) are the reaction rate constants with values of 0.89, 5.01×10^{-4}, and 6.6×10^{-7} mol m^{-2} s^{-1}, respectively at 25 ℃; a_{H^+} and $a_{H_2CO_3^*}$ are the activities of H^+ and H_2CO_3* (carbonic acid) in the aqueous phase, respectively; K_{eq} is the equilibrium constant; and IAP is the ion activity product of the reactants/reaction products, defined as $a_{Ca^{2+}} a_{CO_3^{2-}}$ [87]. The reaction rate depends on pH under acidic conditions and becomes nearly constant above a pH of approximately 7.

The mineral dissolution rates for various minerals have been broadly investigated in laboratory and field experiments. Laboratory research on the kinetics of mineral dissolution is mainly conducted with batch, well-mixed flow-through reactors and column experiments ranging from millimeter to meter scale [88]. When using Eq. (2.8) to calculate the mineral dissolution rate, both the composition of the solutions and the mineralogy of the soil are required. Conversely, weathering rates in the field are generally quantified based upon the observed mineral depletion fronts or the water chemistry, which is normalized on the mineral surface area over meters to kilometers of the flow path of the water [89]. Dissolution rates can differ significantly in different mineral and solution systems, and fluctuate with measurement scales. Model predictions using laboratory rate constants are often inconsistent with measured mineral dissolution profiles [90], with laboratory-determined rates up to 4–5 orders of magnitude higher than the rates estimated from natural subsurface systems [91]. For instance, White et al. [92] reported that plagioclase dissolution rates computed from field data at Merced (10^{-15} to 10^{-16} mol m^{-2} s^{-1}) and Davis Run (10^{-16} to 10^{-17} mol m^{-2} s^{-1}) were approximately four orders of magnitude lower than those estimated in the laboratory at pH 7.

The main governing factors that contribute to mineral dissolution rates have been quantified using laboratory experiments, including flow

velocity, mineral composition, and column length [88]. When flow velocity is raised by two orders of magnitude at the column scale, dissolution rates vary by more than two orders of magnitude. Further, dissolution rates in short columns are higher than those in long columns with the same mineral distribution under the same conditions of flow velocity [93]. From laboratory studies to field systems, the rate of mineral dissolution is affected by preferential flow paths associated with the heterogeneity, secondary mineral precipitation, contact between soil minerals and percolating solution, and the associated active mineral surface area [94,95]. The pH values may also vary with the mineral dissolution. Other possible factors, such as the saturation condition of reactive fluids or the age of reacting minerals, require further investigation [96]. Additionally, hydrologic heterogeneity can complicate the time-dependent evolution of the rates of mineral dissolution as part of a long-term geochemical process [97].

2.4.2. Biochemical reaction rate

In the past decade, biochemical reactions in groundwater have drawn increased attention owing to their environmental importance, particularly related to human health. Processes such as the mobilization and transport of toxic arsenic or microbially-mediated nitrogen cycling involve microorganisms that participate in biological attenuation or degradation of contaminants [98]. Indeed, contaminant degradation and removal from aquifers heavily depend upon bio-attenuation, particularly that of organic pollutants. Therefore, modeling biochemical processes is critical for evaluating and predicting reactive solute transport and bioremediation strategies in the environment [99].

Commonly used kinetic models for characterization of biological decay reactions include zero-, first-, and second-order models, instantaneous reaction kinetics, and Monod or Michaelis-Menten reaction kinetics [100]. Under some conditions, the assumption of zero- and first-order kinetics is invalid, producing biased degradation rates. Considerable deviations of instantaneous reactions from kinetics are expected in the 'near source' and 'initial period' space–time region [11]. Although numerically more complex to implement, the Monod equation has become the most common empirical reaction model for simulating the growth of microorganisms, in particular for hydrogen-producing bacteria [101]. For a specific strain, the specific growth rate μ (h^{-1}) is related to the growth-limiting substrate concentration S (g/L) and is expressed as [102]:

$$\mu = \mu_{max}\frac{S}{K_S + S} \tag{2.10}$$

where μ_{max} represents the maximum specific growth rate, K_S is the Monod half-saturation constant or substrate concentration with half of the μ_{max} (g/L). This equation can be applied to several substrates. The variation for biomass X (g/L) and substrate S (g/L) concentrations with time in a batch bioreactor can be summarized by:

$$\frac{dX}{dt} = r_X = \mu_{max}\frac{S}{K_S + S}X \tag{2.11}$$

$$\frac{dS}{dt} = r_S = -\frac{1}{Y_{S/X}}\mu_{max}\frac{S}{K_S + S}X \tag{2.12}$$

while $Y_{S/X}$ is described as the mass of biomass decay in a unit mass of substrate (g/g). During solute transport modeling, the mass balance equation reactions can be coupled through source/sink terms in the reactive transport equation [103].

A variety of studies have investigated reaction rate discrepancies at different scales. The studies revealed that the time to reach chemical equilibrium, the degree of mixing, and the mass ratios of substrate saturation all vary between the laboratory and the field scale. The field-observed rates are often an order of magnitude lower than those observed within laboratory microcosms [104]. Thus, field models with laboratory-derived parameters generally overestimate mass transfer from biological reactions [105]. In the field, lower reaction rates (and therefore lower remediation efficiency) are attributed to the complex interactions among physical, chemical, and biological heterogeneities in two types. The intrinsic factors include spatial variations in microbial species, active bioavailability, and the distribution of biomass [106]. The extrinsic factors are those related to hydrological and microbial processes [107].

2.5. Equivalent parameter, effective and macroscopic parameter

Three terms often appear to be related in the context of upscaled parameters: "equivalent" parameter, "effective" parameter, and "macroscopic" parameter. Consider a large domain that is discretized into blocks, and a specific parameter (e.g., K) is defined in each of them. When heterogeneity exists between the blocks, a bulk conductivity value may be defined that reproduces the overall behavior of the domain while still maintaining the local block behavior. A resulting upscaled parameter determined in this way is based on a macroscopic form of Darcy's equation and is called an equivalent parameter. Equivalent parameters are thus related to a certain geometry and are spatial averages based upon a single realization. The determination of equivalent parameters is as well linked to the selection of boundary conditions. Some alternative definitions may be required to incorporate the effects of boundary conditions after putting the block back into the aquifer [108]. Contrarily, in heterogeneous media, the values of effective parameters represent the mean behavior via a set of realizations, which are based on the method of moments [109].

In addition, the part of heterogeneity that is not reflected in the model is as well accounted for in the macroscopic parameters. As a result, they are often adopted with the corresponded effective hydraulic conductivity [110]. The spatial and ensemble averages in stochastic modeling are interchangeable since the transport is ergodic, which implies that the solute cloud can sample all the heterogeneous structures as it is far greater than the characteristic scale of heterogeneity. Therefore, the parameter definitions approach the same value for very large geometries under the assumption of ergodicity. In recent research studies, these terms are not clearly distinguished and are often treated as synonymous.

3. Traditional and novel deterministic upscaling of K and k

3.1. Spatial averaging in Darcy's scale

Spatial averaging is one of the most easily implemented concepts across Darcy's scales. The conductivity of each block at a coarse scale is estimated as an average value over its enclosed high-resolution grid cells at finer scales. Power law averaging is a widely used method to calculate the parameters, expressed as [111]:

$$K_{\mathrm{V}} = \left(\frac{1}{\mathrm{V}}\int_{\mathrm{V}} K(\mathbf{x})^p d\mathrm{V}\right)^{1/p} \tag{3.1}$$

where V represents the block value and p is the power averaging exponent, which is related to the permeability structure and bounded from -1 to 1. For $p = 1$, the calculated parameter is equal to the arithmetic mean corresponding to flow parallel to a layered structure. For $p = -1$, the parameter is equivalent to the harmonic mean associated with flow perpendicular to a layered structure. Eq. (3.1) yields the geometric mean when p approaches zero, which has been applied for finite blocks without much justification [112]. A fundamental part of the method is determining the scaling exponent p. The averaging with geometric, arithmetic, harmonic, harmonic-arithmetic, and arithmetic-harmonic means are tested and compared with different hydraulic conductivity settings, including uncorrelated and correlated, isotropic, and anisotropic, and binary distributions [113]. The results showed that for all heterogeneous formations, no simple average is found to be valid.

Therefore, apart from being case-specific, the optimal exponent p is also a function of the heterogeneity characteristics as well as block shape and size [114]. Detailed numerical experiments are recommended to select the most appropriate p-value in practical applications.

Note that the block conductivity is only related to the conductivity within the block in Eq. (3.1), which is referred to as a local technique. The local method assumes the hydraulic head difference to be additive explicitly as a scalar. Local upscaling only results in estimates of diagonal conductivity or permeability terms in isotropic direction and does not produce off-diagonal terms as it is treated as a scalar instead of a tensor. Another widely used local upscaling method is renormalization, which computes equivalent conductivity or transmissivity with an iterative procedure [115]. From a computational point of view, it is one of the most efficient techniques, which is very cheap and can easily be implemented into a numerical code.

Under a non-linear flow condition, local upscaling can be affected by the flow conditions within the block induced by boundary conditions. If the flux in the block is considered as a uniform flow, then the block conductivity can be expressed as [33]:

$$K_V = \int_V \mathbf{q}(\mathbf{x})d\mathbf{x} \Big/ \int_V \nabla h(\mathbf{x})d\mathbf{x} \tag{3.2}$$

where $\mathbf{q}(\mathbf{x})$ and $\nabla h(\mathbf{x})$ are the flux and hydraulic head gradient at the measurement scale respectivity.

Different from Eq. (3.1), the block conductivity in Eq. (3.2) depends not only on the local conductivity but also on the flow field, which in turn is recognized as a non-local or global technique. Global upscaling not only accounts for the heterogeneity inside the upscaled region but also incorporates the global impact from the entire domain. It is crucial to address the challenges associated with flow parameter upscaling, especially when establishing accurate boundary conditions. The boundary conditions describe the interactions between groundwater, surface water, and recharge, among others. The upscaled parameters directly depend on the assumptions that are made in relation to boundary conditions. Accordingly, inaccurate flux exchange across boundaries and the hydraulic head on a fine scale and a coarse scale, respectively, may introduce additional errors. These kinds of errors are critical relative to those introduced by inaccurate heterogeneity upscaling, and the reduction of such errors has been shown to improve upscaled models by up to 70% [116]. Therefore, when attempting to forecast groundwater heads, the accurate upscaling of boundary conditions is significantly more important than hydraulic transmissivity. However, global upscaling is computationally expensive. In some cases, it is not feasible to solve the entire domain on fine scales due to excessive memory that is required [117].

Notably, Eqs. (3.1) and Eq. (3.2) are applied only in isotropic cases. It can be extended from isotropic formations to anisotropic ones to produce tensorial equivalent conductivity [118]. In the case of statistically anisotropic conductivities, elements of the upscaled conductivity tensors are computed by applying the averaging method in the three principal axes directions independently, given that their principal directions are known. In practice, especially in the field, most aquifers are assumed to be isotropic to reduce computing costs associated with upscaling. It is well-established that the errors generated from assumed isotropy are small compared to the total errors introduced by scaling [119].

3.2. Fractal geometry across scales

Fractal geometry has elicited much interest in the field of natural science. The term fractal refers to any geometric object that possesses a fractal dimension greater than its topological dimension [120]. A crucial feature of a fractal structure is its scale independence, which makes upscaling an irrelevant but appealing challenge [121]. Porous and fractured media in nature are interconnected systems in which the distribution of pores or fractures might follow invariant property scaling and be treated as fractals [122]. Fractal geometry was adopted into the field of hydrogeology as early as the 1980s to describe the shape of irregular groundwater flow and transport paths in subsurface media by measuring their fractal dimension. The measure of a fractal parameter such as flow, $M(L)$, is determined by the length scale, L, over a power-law scaling [123].

$$M(L) \sim L^{Df} \tag{3.3}$$

where M denotes the feature of an object, such as length, area, volume, or mass, and D_f represents the fractal dimension. In porous media, the grain mass, pore volume, pore surface, the surface of rocks, fault length, velocity surface roughness, particle size, fragmentation, and connectivity may all potentially follow a single fractal dimension similar to the form shown in Eq. (3.3) [124]. The fractal dimensions are often obtained from measurements within a limiting scale and have been collected for various soils and rocks in previous studies [125].

Diverse groundwater flow and transport variables can be obtained through fractal analysis. Based on the pore microstructures, it is feasible to upscale the hydraulic conductivity in porous media [126]. Various forms of fractal models are derived in terms of different effect factors [127]. Some of the equations are consistent with the Kozeny-Carman (KC) model, while others still require testing with precise observations. By defining a time- and space-dependent dispersivity in the form of a separable power-law, Su et al. [128] developed fractal equations for solute transport in saturated heterogeneous porous media. Wheatcraft and Tyler [129] approximated the dispersion in porous media as a set of fractal stream tubes and developed an expression for scale-dependent dispersivity with Lagrangian models. Meanwhile, O'Shaughnessy and Procaccia [130] proposed a generalization of the diffusion equation for Euclidean lattices in the absence of an advection term. The mineral dissolution rates associated with the roughness of solid surfaces were investigated to estimate the reaction rates within fractures [131]. Many researchers have found that isothermic adsorption is dependent upon the surface's fractal dimension and thus endeavor to improve isothermal predictions. In such works, the fractal models are constructed through modification of the classic Langmuir or Freundlich isotherms, where the geometric characteristics of the solute are linked to surface roughness [132] or the amount of adsorbed mass [133]. Additionally, the results demonstrate power-law dependence in the effective reaction order with time, suggesting a need to investigate the temporal upscaling issue in the future.

3.3. Wavelet transformations

The wavelet transformations (WTs) method coarsens the computational grids by preserving the significant spatial distribution characterizations of the parameter fields and averaging out those that have limited contributions to the flow pattern. Therefore, the grid resolution and the associated computing effort are drastically downsized without neglecting important information. The scaled model provides an overall acceptable description of the flow field and comparable results but with largely reduced computational cost [134]. Considering the spatially varied parameter $K(\mathbf{x})$, the WT of $K(\mathbf{x})$ is denoted as the *wavelet detail coefficient,* by [135]

$$D(a,\mathbf{b}) = \int_{-\infty}^{\infty} K(\mathbf{x})\psi_{ab}(\mathbf{x})d\mathbf{x} = \frac{1}{\sqrt{a}}\int_{-\infty}^{\infty} K(\mathbf{x})\psi[(\mathbf{x}-\mathbf{b})/a]d\mathbf{x} \tag{3.4}$$

where $\psi(\mathbf{x})$ is called the mother wavelet, a is a rescaling parameter, and $\mathbf{b}$ is the translation of the wavelet. Varied forms of mother wavelet functions provide flexibility in capturing the spatially distributed features of $K(\mathbf{x})$. By evaluating the WT of $K(\mathbf{x})$ using a shifted or rescaled wavelet, one can analyze the spatial distribution of $K(\mathbf{x})$ at different length scales of interest. Moreover, numerous grid cells can be integrated into one large block if they share proximate information of $K(\mathbf{x})$ and without the need of a detailed expression in each cell.

In geoscience, $D(a,\mathbf{b})$ contains information that is lost between two approximations of $K(\mathbf{x})$ at two *successive* length scales. The reserved information at a fixed scale is given by a scaling function, $\varphi(\mathbf{x})$. The *wavelet approximate* or *wavelet scale coefficient is* defined by

$$S(a,\mathbf{b}) = \int_{-\infty}^{\infty} K(\mathbf{x})\phi_{ab}(\mathbf{x})d\mathbf{x} \tag{3.5}$$

In general, upscaling by the WT method is non-uniform. Therefore, an appropriate numerical approach suited for the unequal blocks in the geological model is needed. The numerical models could be established based on the analogy between electrical and currents. Another effective method is to reconstruct f(K) by computing its inverse WT after setting some of the scale and detail coefficients to zero. The effective permeabilities of the upscaled blocks then can be derived from the reconstructed f(K). The difference between these two methods was found to be negligible by Rasaei and Sahimi [135].

The WT method has recursive properties, meaning that it can be repeatedly applied and compressed a set of data multiple times in the same region until an efficient coarsening has been conducted for generating the final upscaled grid. The WT method is ideally suited for the regions with unevenly distributed potentially high or low permeable sectors, which require non-uniform coarsening. The efficiency of the WT method increases as permeability distributions broaden, as well as the upscaled model accuracy [136]. For example, only a small fraction of preferential flow paths significantly contribute to flow through highly heterogeneous media. Therefore, the upscaling can focus on the properties where the preferential flow occurs.

3.4. Physically-based methods in pore networks

Percolation theory (PT) is a fundamental component of probability theory that presents phase transitions in all dimensions. Such transitions are termed critical phenomena [137], wherein the physical behavior of a system undergoes drastic changes near a particular point. In percolation theory, a porous medium is treated as a pore network (PN) consisting of pore throats and pore bodies to represent flow paths as well as flow resistance in porous media. With phase transition, PT allows developing formulations for flow and transport properties as functions of the scaling structure of their geometric features. Many percolation properties follow power laws in the vicinity of the so-called percolation threshold or critical percolation probability, p_c. At this critical point, the system behavior changes significantly. The exponents in the power laws are independent of the porous medium morphology and are only dependent on the spatial dimension d as a universality class. In general, the number of finite clusters $n_s(p)$ in each site near p_c follows the relation

$$n_s(p) \propto s^{-\tau} F[c(p)s], s \to \infty \tag{3.6}$$

where τ represents a free exponent and F denotes a scaling function. Near the percolation threshold, $c(p)$ is allowed to behave as a general power-law, $c(p) \propto |p\text{-}p_c|^{-1/l}$, where l is another critical exponent [138]. For applying PT to upscaled permeability, Sahimi [139] summarized several intrinsic relationships of percolation exponents relevant to geometric properties near the p_c. For example, the critical behavior of the permeability K of an infinite system is defined by

$$K \propto (p - p_c)^{\mathrm{k}} \tag{3.7}$$

where k is determined by $\mathrm{k} = \varsigma_k + (d-2)\nu$. The system's dimensionality is the sole determinant of the exponents. For a two-dimensional system, $\mathrm{k} \approx 1.3$ [140], while for a three-dimensional system, $\mathrm{k} \approx 2$ [141]. Therefore, the consistency of the power provides universal characterization to estimate the geometrical or physical properties of a medium, which is also its principal advantage [142]. It should be noted that percolation scaling applies only near the percolation threshold and that only the impact of spatial correlation information on p_c is integrated into the upscaling of K [143].

The critical path analysis (CPA) is a physically-based analysis with similar concepts to PT. In the context of CPA upscaling of K at the pore scale, if the size of all the pores in a media is gradually decreased, the last pore that completes a connected path is considered the "critical" pore. The associated smallest conductivity corresponding to the critical pore size is assigned as critical conductivity, Kc. According to CPA, other pores smaller than the critical pore do not noticeably influence the upscaled value of K. The procedure can be adopted to upscale flow and transport at geological scales, and its application to upscaling at such scales provides a remarkably accurate, non-numerical solution applicable in a wide range of circumstances. Further, if low-permeability zones are eliminated from the porous medium, CPA is reduced to a simple percolation system [23].

To implement CPA to model permeability in a porous medium, a relationship between specific pore shape and geometrical characteristics must be assumed. Katz and Thompson [144] estimated the permeability of rocks from the critical pore diameter and formation factor by presuming a linearly cylindrical pore diameter variation with its length. Bernabe and Bruderer [145] derived a similar expression of the saturated hydraulic conductivity in the form:

$$K = \frac{r^2}{cF} \tag{3.8}$$

where r is a length related to pore geometry and c is a constant coefficient equal to 8. When calculating absolute permeability (k), c is instead equal to 226 [146]. Using Eq. (3.8) requires the determination of F, a formation factor that depends on electrical conductivity and gives the ratio of the fluid bulk conductivity to the rock conductivity (excluding surface conduction). The value of F may be estimated from mercury intrusion [146] or water expulsion porosimetry [147]. Therefore, the mode of the pore size distribution can be used to accurately determine r, which is crucial to CPA. Thompson [148] further tested the formula by applying mercury injection to sandstones, carbonates, and metamorphic rocks; estimated permeabilities matched well with measured permeabilities, with values spanning nearly eight orders of magnitude (from 10^{-3} to 10^5 darcy).

Similarly, an estimation of k within a factor of two by utilizing CPA was shown by Ghanbarian et al. [149], compared to tight-gas sandstone measurements. Nonetheless, they used $c = 53.5$, in agreement with [150]. In a different study, Daigle [151] determined k in various types of rocks including clay-rich samples and carbonate by utilizing CPA with c = 32, and showed that the estimates of the CPA model match. They presumed that the power-law probability density function was obeyed by the pore size distribution and that there was a conformation between the formation factor and universal scaling from percolation theory. Friedman and Seaton [152] applied CPA to determine viscous (hydraulic) permeability in 3D pore networks, while Hunt and Gee [153] calculated the unsaturated hydraulic conductivity (K_S) of soils with pore spaces compatible with a fractal description. The CPA method can be used to determine the relationships between other transport characterizations, but not their absolute values (i.e., Knudsen apparent molecular and Knudsen diffusivities [152]).

Compared to the other methods in this section, PT relatively has the potential to upscale the connectivity or effective medium approximation for transport properties [23]. It has been broadened and applied in upscaling a variety of parameters, including thermal conductivities, diffusion coefficients, the distribution of solute arrival time, sorption, and chemical reaction rates [154]. PT can as well be combined with other methodologies, which will be covered in the followed sections to analyze the upscaling of flow and transport parameters, such as continuous-time random walk, fractal laws, and effective medium theories [154]. A specified model is often needed for each application of quantitative prediction of dispersion or the scaling of chemical reaction rates. However, detailed information about the porous medium is not crucial for facilitating a good experimental prediction, but instead, the

connectivity of the flow paths through the medium directly influences the PT parameters [155].

3.5. Machine learning with media images

With the booming computing science industry, artificial intelligence (AI), which encompasses machine learning (ML) and deep learning (DL), has come out as a comprehensive and adaptive tool, reshaping industries and creating an environment for scientific advancement [156]. It also offers a distinct approach for modeling many phenomena involving porous and fractured media. The basic principle of ML is to predict unknown processes by constructing relationships between inputs and the associated outcomes [156]. Detailed information about this approach is depicted in numerous literature [157]. Despite its successful predictions of surface water, the applications of ML in hydrogeology are finite. *Water Resources Research* has recently published a new special issue on "Big Data & Machine Learning in Water Sciences: Recent Progress and Their Use in Advancing Science" [158]. Only limited papers are related to the application in groundwater and bounded in the surface soils. This is because the nature of ML requires big data to drive. High-frequency data in a large spatial area in surface water are more easily obtained and satellite data can be adopted. However, access to groundwater and geological data is constrained and extremely expensive.

Currently, the application of ML in upscaling effective parameters is mainly to solve flow and transport properties that have relationships with the media morphology. The ML method is able to extract pivotal geometrical features from their images, and then estimate correspondent transport parameters with image-based data [159]. Saxena et al. [160] used a convolutional neural network (CNN) to evaluate the effective permeability from their microstructures images. The successful application of CNN on the prediction of permeability provides valued cognizance in understanding the connection between permeabilities and geometric features [161]. The ML method has also been used to estimate the effective diffusivity of 2D porous media from structure images [162], and the application can be further extended to 3D images. Macroscopic permeability was derived by using both artificial neural network (ANN) and deep learning (DL) algorithms with 3D sandstone images [163]. Araya and Ghezzehei [164] developed ML-based pedo-transfer functions to simulate saturated hydraulic conductivity (*Ks*) over 18,000 soils. Meanwhile, the performance of four popular ML algorithms: support vector regression (SVR), K-nearest neighbors (KNN), boosted regression trees (BRT), and random forest (RF), have also been evaluated. The accuracy varied in each ML method, therefore, attentions need to be paid on implementing an appropriate algorithm with high efficiency, high accuracy, low constraints, and affordable computing cost from the ML pool. More applications of ML are as well found in recent literatures. Rao and Liu [165] proposed a 3D, deep convolutional neural network (CNN) to predict the effective material properties of representative volume elements (RVEs) with random spherical inclusions, and showed advantages over the conventional finite element based homogenization regarding uncertainty quantification, computational efficiency, and model transferability. Based upon a similar scheme, Andrianov and Nick [166] learned a set of parameters from fine-scale simulations to a coarse-scale grid block in a fracture geometry via a CNN.

During implementation, several key steps are typically followed. First, porous images are used as input to generate a training database between porosity and effective conductivity or diffusivity, which can be obtained experimentally or numerically for porous or fractured media. A training model is then established and validated by using the dataset with an ML method in the next step. Finally, the trained model can be cast to predict the effective transport attributes of new porous media without repeating the training process. It has been shown that the features extracted with ML are more accurate and efficient than geometric measurements and are unconstrained by human pre-conceptions. Furthermore, if new physical characteristics of porous media are found to influence effective permeability, it can easily be upgraded [163].

The disadvantage is always the effort to build the training realizations. Gathering enough sizable images is expensive, especially for 3D images from micro-CT scans. Though the DL method is popular and fancy, it is better to balance the two sides when adopting this method for real-world application. Meanwhile, the current methods are only valid for the scale we can sample and analyze (e.g., core scale), and implementing the methods from core scale to field scale is still a challenge. Currently, DL is still in the initial "value discovery" phase in hydrogeology science. However, with improvements in subsurface real-time monitoring systems, DL could contribute to a wide spectrum of issues in the field by harnessing big data and ML through collaboration with computer scientists.

4. Generalized theories for multiple parameters upscaling

4.1. Homogenization theory

Homogenization encompasses a very broad area and requires periodic structures of porous media for parameters upscaling. Consider a macroscopic domain, it can be described as consisting of a collection of circular, periodic microscopic cells as shown in Fig. 7. In a periodic medium, the period size is much smaller than the medium sample size. Homogenization is the process of seeking an averaged formulation by describing the periodic array with an asymptotic analysis [167]. The selection of an appropriately small scaling parameter is one of the basic requirements for implementing the approach [168]. Generally, the homogenization theory applies to partial differential equations with rapidly fluctuating coefficients at various scales.

For a porous medium, the ratio of the microscopic period $\times$ and macroscopic length y can be characterized as a spatial scale metric ε, where $\varepsilon = x/y$. From limit theory, homogenization upscaling seeks a slowly varying or constant coefficient to substitute the rapidly oscillating coefficients in an asymptotic transition manner from microscopic to macroscopic scales as ε approaches zero. The upscaled coefficients at the coarse scale should meanwhile satisfy the initial differential equations [170]. For example, two-scale homogenization describes sequences of oscillating functions and proves the convergence of homogenization processes [167]. If any physical quantity Q is treated as a function of two spatial scales, x and y, it can be formally expanded as a power series with the small, dimensionless parameter ε as

$$Q = Q_0(x, y) + \varepsilon Q_1(x, y) + \varepsilon^2 Q_2(x, y) + O(\varepsilon^2) \tag{4.1}$$

As formulated, Q can represent many fluid flow properties, including velocity, diffusion, species concentration, and hydraulic head. The homogenization equation methods determine the equations on a larger scale from constituent equations of a given scale. The parameters are upscaled with equations simultaneously, which requires complicated mathematical derivation. This procedure requires deriving the equation for each specific problem, and various homogenization frameworks have thus been developed, including the energy method of Tartar [171]. Such frameworks are elegant in that they work for different kinds of disordered media, not just for periodic media [172].

Homogenization theory has been successfully applied to a wide variety of groundwater flow and solute transport problems. Though natural porous media are not truly periodic, they can be approximated by neglecting variability at larger scales. Aside from upscaling, it has been adapted to solve the convection–diffusion equation, general nonlinear diffusion equations [173], two-phase flow including time scales [174], fluid flow in porous media with a nonlinear term of heat exchange in the boundary transmission conditions [175], slightly compressible subsurface physics [173], and adsorption–desorption processes [176]. In order to apply this in fractured media, an upscaled model was derived by Sahimi and Bruining [23] for vertically fractured reservoirs, including

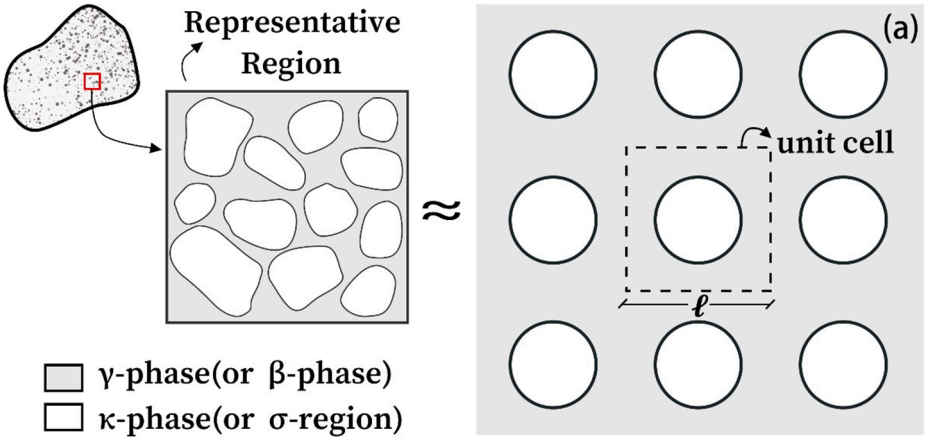

Fig. 7. Spatially periodic models of porous media with a two-dimensional array of cylinders (revised based on da Silva et al. [169]).

relative permeabilities and capillary pressures with non-equilibrium effects. Further, it has been adapted to scale the bacterial-sized effective nutrient diffusion uptake as well as other microscale properties in accordance with first-order uptake kinetics through a locally periodic array of spherical bacteria. The flow in carbonate rocks consisting of complex geological structures like solution-collapse breccias and fractures was described by Lopes et al. [177] by using a novel three-scale (micro, meso, macro) computational model. Their model was developed based on a homogenization procedure that was reiterated by the substitution of equivalent continua with computed properties from homogenization schemes that are self-consistent.

Alongside the requirements for scale separation and geometry periodicity, another two implicitly assembled assumptions are made when applying periodicity: stationarity of conditions and local equilibrium. Thus, while homogenization is valid to recover an asymptotic stationary macroscopic model, it is not reliable for processes with long transition times or lengths. For example, mixing has a long pre-asymptotic period, and thus homogenization might produce inaccurate results for evaluating its initial variations. Compared to the spatial averaging method, which smooths and averages properties within a volume, homogenization upscales by allowing the microscale approach to zero. An appealing feature of homogenization is that a closure scheme is not required to construct the transport equations at the macroscale, as is required for volume averaging [178]. Homogenization is not limited to generating emerging macroscopic equations but rather is a rigorous and robust analysis of the multiscale features of the model that should be recommended in practical applications.

4.2. Method of moments

The method of moments is a statistical approach to estimate population parameters, such as the mean or variance [179]. The method was initially introduced by Aris [180] and was extended by Horn [181]. In principle, if the population parameter estimates are equal to the moments of a sample, then the statistics of the sample can be estimated and replaced by the population moments in the equations. Therefore, the method can be used to estimate the field-scale/block effective hydraulic conductivity from the local conductivity. Different from estimating the block conductivity from average flow discharge and hydraulic gradient, the method of moments rather finds a block value that is equivalent to the spatial moments of the hydraulic head in the heterogeneous medium [182]. To implement the method of moments, the geological formation needs to be assumed to possess periodic hydrological and geochemical characteristics in all directions. The periodicity means that the associated parameters repeat themselves with a specified period, which is much smaller than the scale of the concerned domain. With the efforts of researchers, the results can now be expanded to more general cases, which will be discussed in a subsequent section.

Macroscopic solute transport is governed by the mean velocity vector and dyadic dispersion coefficients. Expressions can be derived for these apparent coefficients by using the generalized Taylor-Aris dispersion. The application of the method of moments usually includes four steps. First, a governing partial differential equation needs to be formulated with a distribution of head or solute concentration $\phi(t, \boldsymbol{X})$, which is a function of time and space. For an unsteady flow through a 3D, confined, anisotropic, heterogeneous formation of a compressible matrix without sources or sinks, the governing equation is [183],

$$S(\boldsymbol{X})\frac{\partial\phi(t,\boldsymbol{X})}{\partial t} = \nabla\bullet[\boldsymbol{K}(\boldsymbol{X})\bullet\nabla\phi(\mathrm{t},\boldsymbol{X})] \tag{4.2}$$

From the periodic assumption in space, a vector of spatial coordinates $\boldsymbol{X}$ may be expressed as the sum of an unbounded global variable and a bounded local variable [179], i.e., $\boldsymbol{X}=\boldsymbol{X_n}+\boldsymbol{x}$, therefore, $\phi(t, \boldsymbol{X})=\phi(t,\boldsymbol{X_n},\boldsymbol{x})$. Second, the local spatial moments of the hydraulic head or the solute concentration can be defined as [183]:

$$\boldsymbol{m}_p(t,\boldsymbol{x}) = \sum_n \boldsymbol{X_n^p}\phi(t,\boldsymbol{X_n},\boldsymbol{x}) \qquad (p=0,1,2,\ldots) \tag{4.3}$$

where Σ_n denotes the triple summation $\sum_{n_x=-\infty}^{\infty}\sum_{n_2=-\infty}^{\infty}\sum_{n_3=-\infty}^{\infty}$. $\boldsymbol{X_n^p}$ is a coordination-related term and known as a p-adic. The corresponding moments are determined by the value of p. For example, if $p=0$, $\boldsymbol{X_n}=1$. The zeroth moment $m_0(t,x)$ is then the sum of the variables at all points of the domain with local coordinates x; for $p=1$, $\boldsymbol{X_n^1}$ is a 3D vector of coordinates indicating the origin of the nth unit element; for $p=2$, $\boldsymbol{X_n^2}$ is the second-order tensor whose ijth element is the product of the i and j element of $\boldsymbol{X_n}$, and so on [184]. Correspondingly, the global moments are then defined as the integral of local moments over the local domain [183].

$$\boldsymbol{M}_p(t) = \int_{V_0}\boldsymbol{m}_p(t,\boldsymbol{x})d^3\boldsymbol{x} \qquad (p=0.1,2,\ldots) \tag{4.4}$$

where V_0 denotes a unit element domain and d^3x represents a differential volume in the unit element. Third, a governing equation in terms of the local moments as variables needs to be generated. This can be derived by multiplying Eq. (4.2) by $\boldsymbol{X_n^p}$ and summing them together with the overall unit elements, the result is the rate of change of the local moments, which reaches a steady state and equals zero [183]. The derived equation is expressed as,

$$S(\boldsymbol{x})\frac{\partial\boldsymbol{m}_p(t,\boldsymbol{x})}{\partial t} = \nabla\bullet\left[\boldsymbol{K}(\boldsymbol{x})\bullet\nabla\boldsymbol{m}_{\mathrm{p}}(\mathrm{t},\boldsymbol{x})\right] \tag{4.5}$$

Last, the zero-, first- and second-order global moments are obtained with the solution of the local moments since certain boundary

conditions imposed at the surfaces of the unit element are satisfied by the local moments [185]. The zero-order moment (M_0) is a scalar that characterizes the total change in the hydraulic head or solute concentration. Here, it is also assumed that there is a gradually varying flow, which suggests that the hydraulic head fluctuations have a correlation length that is larger than that of the local hydraulic conductivity and specific storage fluctuations [186]. The first-order moment is a vector where the ratio M_1/M_0 represents the location of the centroid of the distribution and the second-order moment is the matrix of dyadic where M_2/M_0 indicates the mean square deviation of the distribution. By defining the effective parameters in terms of the global moments under local equilibrium conditions, we can finally have the expression of the effective asymptotic parameters [187], such as the macrodispersion in [179].

$$D^* = \frac{1}{2}\lim_{t\to\infty}\frac{d}{dt}\left(\frac{M_2}{M_0} - \frac{M_1 M_1}{M_0^2}\right) \tag{4.6}$$

Kitanidis [188] derived general expressions for effective conductivity by solving the first spatial moment of the solute concentration in heterogeneous porous media with random time-invariant flow velocities. The expressions of macrodispersion of sorbing solutes are investigated, and it was found that a second term and a third term were integrated by the longitudinal macrodispersion, and these terms account for the effect of averaging the distribution coefficient and the first-order sorption rate in the equilibrium and kinetic sorption relation, separately [185]. Field formations exhibit recurrent geochemical characteristics which are not absolutely periodic, and as such, a porous medium that is assumed to be geochemically spatial and periodic may be criticized. Mathematically, it is beneficial, as it can be used to obtain expressions that are exact. Apart from the ease in representing spatial repetitiveness, the periodic model can also be used in the more general stationary case to obtain results as an intermediate step, as demonstrated by Kitanidis [189] for the hydraulic conductivity case.

Schemes based on the method of moments have already been proposed in the literature for formulating an effective equation and calculating the effective coefficients appearing therein to study the influence of multiple reactive processes on contaminant transport and fate across multiple scales [190]. Effective velocity, effective dispersion coefficient, and effective sorption rate at the macroscale are all investigated in the upscaled moment equation. Kitanidis [189] derived general expressions for effective conductivity by solving the first spatial moment of the solute concentration in heterogeneous porous media with random, time-invariant flow velocities. The expressions of macrodispersion of sorbing solutes are investigated and found the longitudinal macrodispersion integrates a second and a third term that represents the effect of distribution coefficient averaging and the first-order sorption rate in the equilibrium and kinetic sorption relation, separately [185]. By modeling the periodic medium as a discrete graphical network, the method is applied to homogenize the resulting global equation to explicitly express the effective solute velocity, the effective first-order irreversible reaction rate constant, and the effective dispersivity dyadic [191].

Other processes, such as sorption and matrix transport, are further derived with the method of moments for coupled transport with reactive species [185]. Moment analysis is also adapted to characterize the distribution of active microbial biomass and contaminants in aquifers and to calculate the field scale Monod parameters through the inverse coupling method [192]. The restrictiveness of periodic boundary conditions may be less intuitive and has been addressed in the companion paper through several examples and by comparison with other methods which make different assumptions [193]. However, the moment computation for arbitrarily heterogeneous media is not always well understood [194] and a considerable amount of data is needed for the calculation of concentration moments. For a more general case of stationary random porous media, Vikhansk [195] developed an extended method of moments that allows the calculation of moments beyond the classical second-order. The generated higher moments allow quantifying the deviations from the solution predicted by the advection–diffusion equation for averaged concentration.

4.3. Volume averaging

Volume averaging is a method to upscale a wide range of groundwater flow and transport parameters, including conductivity, dispersivity, and reaction coefficients. The fundamental idea of volume averaging is to upscale the solute transport governing equations at the Darcy-scale in a closed volume [196]. Application of this method requires the making of various assumptions. First, the heterogeneous reservoir is treated as a combination of multiple homogeneous parts (i.e., different regions for pores and solids, different facies for mineral types, or different phases for fluid and biofilm). Second, the hierarchical structure or relationship between the parts is already known, and the conventional mass balance equation can be written for each of the homogeneous parts. Third, the reservoirs are statistically stationary with no strong changes. This is because when putting the averaged volume back into the reservoir, the volume fractions of each facies within the averaging volume do not change. In this way, hierarchical transition probability theory can be used to express relationships between property structures at different scales, enabling the representation of scale-dependent parameters such as matrix diffusion coefficient, fracture aperture, reaction rate coefficients, and dispersivities as functions of spatial scale [197].

To implement the volume averaging method, superficial and intrinsic volume averaging operators are defined [198]:

$$\langle \psi_k \rangle = \frac{1}{V}\int_{V_k} \psi_k dV \tag{4.7}$$

$$\langle \psi_k \rangle^k = \frac{1}{V_k}\int_{V_k} \psi_k dV \tag{4.8}$$

The relationship of the averaging operators and the volume fraction of the k-region can be depicted as:

$$\langle \psi_k \rangle^k = \varepsilon_k \langle \psi_k \rangle^k, \varepsilon_k = V_k/V \tag{4.9}$$

where V and V_k represent the total and k-region encompassed geometrical spaces, respectively. ψ_k denotes any concerned variable in the k-region. In a multi-facies geological reservoir, k is the k-th facies region [199]. In a porous medium encompassing a solid matrix and a void, k represents the porous particle phase or fluid phase, separately [200]. In a porous medium colonized by biofilms that include biologically-mediated reactions, k represents the mass conservation in the fluid and the biofilm [201].

As the derivation of the upscaled model involves significant algebraic effort which varies from case to case and may discourage non-specialists, the interested reader is referred to the detailed mathematical development in the above literature. The volume-averaged equation for transport in porous media with mineral surfaces can be derived by applying the volume averaging operators to the advection and dispersion terms in the multi-regional groundwater flow and transport equation. To successfully smooth the variable in space, the appropriate shape and size of the averaging volume need to be chosen carefully. Aguilar-Madera et al. [202] used the volume averaging method to estimate effective coefficients in a one-equation model for solute transport in heterogeneous reservoirs. The closure schemes which support the calculation of the effective coefficients for varied arrangements of lithologies and sediments are illustrated in detail in [199]. Notably, the method often generates an array of unknown variables in representative geometries. In a reservoir containing k well-defined geological facies: a number of k^2 for ordinary and crossed dispersive coefficients; k^2 for conservative and non-conservative ordinary and crossed pseudo-velocity, respectively; k for pseudo-absorption coefficients; $k + 1$ for mass transfer coefficients;

and the mass interchange coefficients are introduced into the developed averaged equations. These effective coefficients can be interpreted by considering the geometrical distribution of facies and associated physical mechanics that interplay at a small scale [199]. If the representative geometries of the reservoir involve boundary-value problems, the effective coefficients need to be recalculated based on the realistic study region.

The volume averaging technique with closure has been successfully used to determine the effective dispersion tensor for homogeneous [203] and heterogeneous [204] porous media. The applications for upscaling reactive transport processes involving bimolecular reactions are investigated from the laboratory to the field scale [196]. Two limitations, one associated with the determination of the increased coefficients and another with the solving of the boundary constrained model, largely hinder the application to the heterogeneous subsurface. The extension to reservoirs with more than three facies is theoretically derivable but overwhelmingly complex. The multi-facies equations will yield much more averaged equations and effective coefficients than the two-facies equation. Generally, validation requires simplified geological parameters, such as lenticular and layered reservoirs [199] or reversible liner heterogeneous chemical reactions in an in-line arrangement of spheres [205].

The volume averaging operators may also be applied to the mass transfer coefficient. Leung et al. [194] assessed the scaling characteristics of effective mass transfer coefficient for non-reactive solute transport. Dai et al. [64] upscaled the diffusion coefficient for multimodal fractured heterogeneous rocks from the laboratory to the field scale. By considering the diffusion coefficient (D_m) as lumped and spatially random, they used the matrix porosity and fracture aperture to estimate the mass transfer between the fractures and the matrix. The scale dependence of D_m is related to heterogeneity in physical and chemical matrix properties both within and across matrix units. The spatial-scale dependence of the effective D_m can be derived by constructing a covariance function of $\ln(D_m)$ with heterogeneous matrix properties characterization, assuming that the variance is smaller than unity. At the field scale, the effective D_m is controlled by both the domain size and laboratory-scale $\ln(D_m)$ statistics (i.e., geometric mean, variance, and integral scale). Its value is larger than the geometric mean of $\ln(D_m)$ and increases with the integral scales. The algorithm may be simplified for unimodal and bimodal distributions and can be used to upscale other effective parameters (i.e., effective retardation factor, effective sorption coefficient) [206]. The drawback of this approach is that its application has been only tested with synthetic Monte Carlo simulations and has not yet been applied to experimental or site collected data. The next extension of the effort will be to validate the volume averaging method by using observed data, and to incorporate the influence of other processes that influence mass transfer, such as spatial variations in aperture size and matrix porosity.

5. Stochastic upscaling and implementations

5.1. Classical stochastic formulations

In deterministic methods, the accuracy and robustness of a model could be improved by incorporating all the available field characterizations and fitting its results to the history observations. However, the uncertainties are still inhered in any geoscience modeling. A popular approach is to acknowledge the fact that the subsurface information cannot be completely acquired and uses a "process-based" model instead of a single realization to represent the uncertainties of a partially characterized formation with geostatistically valid results [207]. In the stochastic approach, the essential is to solve ensemble-average equations of flow and transport with macroscopic variables, such as porosity, conductivity, and dispersivity. Theoretical analysis from both the Eulerian and Lagrangian perspectives have been developed to describe the spreading of solutes; see, some pioneered work by Gelha and Axness [208]. These theories lead to the derivation of effective large-scale parameters, which corresponds to the upscaling of parameters over different scales of interest. In applications, the two methods tend to be equivalent and give similar results [209].

5.1.1. Perturbation theory

Calculations of the ensemble moments, whether in the spectral domain or the actual physical domain, are adaptations of the perturbation theory. We will take the integral spectral method as an example to illustrate how the perturbation methods incorporate upscaling. The equation for the ensemble-average variables in the spectral perturbation method is developed in terms of a perturbation series expansion. It decomposes a stationary random variable into two parts: a constant ensemble average (bracketed value) and random perturbations with a mean of zero (marked value) caused by variability in the parameter field. For transient solute transport through a heterogeneous medium, the pertinent variables, concentration, and velocity are then expressed as $c=\langle c\rangle+c'$ and $u=\langle u\rangle+u'$ [24]. Removing the reaction terms, the governing Eq. (5.1) for the mean concentration can be expressed as [210] (The accuracy of stochastic perturbation solutions to subsurface transport problems)

$$\frac{\partial\langle C\rangle}{\partial t}+\frac{\partial\langle u_i\rangle\langle C\rangle}{\partial t}-\frac{\partial}{\partial x_i}\left(D_{ij}\frac{\partial\langle C\rangle}{\partial x_j}\right)=\frac{\partial}{\partial x_i}\langle -u_i'C'\rangle \tag{5.1}$$

The term $\langle -u_i'C'\rangle$ is the so-called "closure" covariance and reflects additional mass transport due to correlation between the fluctuations of concentration and specified velocity. It generates a macroscopic dispersion effect at a large scale and can be approximated with Gelhar and Axness [210],

$$\frac{\partial}{\partial x_i}\langle -u_i'C'\rangle\approx\frac{\partial}{\partial x_i}\left(D_{ij}^{*}\frac{\partial\langle C\rangle}{\partial x_j}\right) \tag{5.2}$$

If the closure term is evaluated, which is the key for solving the averaged equation, the macrodispersion tensor D_{ij}^* then can be derived. With the ease of governing equations of concentration perturbations when average flow occurs in direction $i=1$, Gelhar and Axness [210] showed D_{ij}^* is proportional to the absolute value of migration velocity, as for the local dispersion tensor.

$$\alpha_L^{*}(t)=D_{L11}^{*}\Big/\langle u_1\rangle=\int\frac{1-\exp(-b\langle u_1\rangle t)}{\gamma^2 b}\left(1-\frac{s_1^2}{s^2}\right)^2 S_{YY}(s)ds \tag{5.3}$$

where $b=2\pi i s_1+4\pi^2\alpha_L s_1^2+4\pi^2\alpha_T(s_2^2+s_3^3)$ and $s=(s_1,s_2,s_3)$ are the Fourier coordinates. S_{YY} expresses the spectral density of the log-permeability field. Eq. (5.3) defines the correlation between macrodispersivity and log-permeability fluctuations. S_{YY},C_{YY} is the Fourier transform of the log-permeability covariance function. The relationship that exists between macrodispersivity log-permeability fluctuations is established by the Fourier transform. An analytical method was developed by Liao et al to approximate numerical solutions in a finite difference scheme with periodic boundary conditions for two-dimensional problems [211]. The method utilizes expansion techniques and Fourier analysis to create explicit formulas of the equivalent conductivity tensor, while heterogeneity and anisotropy of two-dimensional space together with the geometry of grid blocks are considered.

Besides the truncation method, the closure term can as well be approximated by Gaussian [212], random Green's function methods [213], second-order asymptotic expansion approach [214], and Taylor series methods [215]. Li et al. [216] compared these methods and showed similar expressions to the perturbation method. However, the closure covariances in the alternative methods depend on the known deterministic solution rather than the unknown ensemble mean. The perturbations relatively give better accuracy. Further, Li and McLaughlin [216] devised a new spectral approach that can handle nonstationarity but preserving the attractive features of spectral analysis

at the same time. Ginting [217] employed perturbation analysis to derive macro-diffusion.

5.1.2. Lagrangian-based approach

The Lagrangian-based transport model was initially introduced by Dagan [186] to carry out random simulations of solute spread in heterogeneous formations. It regards the solute as a set of indivisible particles which move through the heterogeneous formation driven by fluid convection and diffusion [25,218]. Early studies focused almost entirely on the spatial variation of permeability [53]. Similar to the perturbation theory, macrodispersivity can be characterized by the Lagrangian velocity covariance. Rubin [219] developed the formulas for the univariate and bivariate statistics of ln(k) for bimodal media. Later, the underlying sedimentary architecture was considered to assess the intrinsic natural variability in attributes affecting subsurface transport [8]. The spatial correlation structure in multimodal [220] and hierarchical multimodal frameworks have been developed [221]. The transfer probability is often needed in the framework to estimate the conditional probability of one reactive assemblage occurring at one location while the other reactive facies occur at a different location [197]. Then the solute transport distribution in space and time domains can be calculated by using analytical or numerical integration [222].

An advantage of particle-based methods is that they ignore the restrictions of the analytical methods. These approaches do not require any kind of functional form for the hydraulic properties or the spatial correlation of their structure, and ranges of variability have no restrictions. Lagrangian numerical schemes with local assumptions are flexible as well because the traditional global assumptions such as ergodicity, small global variance, stationarity, or single correlation scale are avoided. Though the assumption is not required here, the concept of covariance is still needed in the formulation.

Considering a domain composed of N mutually exclusive facies defined by ln(k), the corresponding hierarchical (two levels) multimodal mean, variance, and spatial covariance of ln(k) for the whole domain are expressed as [223,224]:

$$m_Y = \sum_{i=1}^{N} p_i m_i \tag{5.4}$$

$$\sigma_Y^2 = \sum_{i=1}^{N} p_i \sigma_i^2 + \frac{1}{2}\sum_{i=1}^{N}\sum_{j\neq i}^{N} p_i p_j (m_i - m_j)^2 \tag{5.5}$$

$$C_Y(h) = \sum_{i=1}^{N}\sum_{j=1}^{N}\{C_{ij}(h) + m_i m_j\} p_i t_{ij}(h) - m_Y^2 \tag{5.6}$$

where $p_i$and m_i are the volume proportion and the mean ln(k) of facies i, respectively. $C_{ij}(h)$ is the spatial covariance within (for $i = j$) or across facies (for $i \neq j$). $t_{ij}(h)$ is the conditional probability for the transition from facies i to facies j with lag distance h, expressed as:

$$t_{ij}(h) = \frac{pr\{I_j(x+h) = 1\}}{pr\{I_i(x) = 1\}} \tag{5.7}$$

where $I_i(x)$ is the space random function (SRF), equal to 1 if facies type i at location x and otherwise equals to 0.

The spatial correlation models developed here can include any number of hierarchical levels (more details available in [225;226]). To evaluate scale-dependent macrodispersivity, Dagan [35] and Rubin [219] calculated the velocity covariance as:

$$\widehat{u}_{ij}(K) = U_1^2\left(\delta_{1i} - \frac{k_i k_1}{k^2}\right)\left(\delta_{1j} - \frac{k_j k_1}{k^2}\right)\widehat{C}_Y(K)(i,j = 1,\cdots,d) \tag{5.8}$$

where u_{ij} is the covariance of velocity between ith and jth facies, the circumflex denotes the Fourier transform operator, δ_{1i} is the Kronecker delta, U_1 is the mean velocity (here, the mean velocity direction is the x direction), k is the modulus of the vector K, and d denotes spatial dimension.

By assuming that the solute particle velocity is approximated as first order, the macrodispersion tensor can be obtained by:

$$D_{ij}(t) = \int_0^t u_{ij}(U_1 t')dt' \tag{5.9}$$

where D_{ij} are the macrodispersion coefficients in the longitudinal (i,j = 1), transverse (i,j = 2), and lateral directions (i,j = 3).

The Lagrangian approach is attractive because it provides a realistic link between geological sedimentary data and solute transport behavior, which gives a better understanding of how the variability in physical and chemical properties at different scales impacts the solute behavior in whole porous or fractural media. The Lagrangian-based model also provides an effective way to address scale-dependent transport parameters [227]. It uses stochastic averaging to incorporate the effects of small-scale spatial variability on solute transport. To consider reactive solute transport undergoing equilibrium sorption within a unimodal porous media, Bellin et al. [228] extended Dagan's classic solution for non-reactive solute transport by incorporating heterogeneity in chemical properties. Rajaram [229] then derived the analytical solution of the scale-dependent effective retardation for unimodal porous media by using the Lagrangian approach and gave an expression for the reactive solutes' Lagrangian velocity and its covariance.

To address the limitation of weak heterogeneity (as occurs when the global log conductivity variance (σ_Y^2) is less than unity) associated with the first-order approximation, Cvetkovic et al. [230] developed physically-based transport models suitable for highly heterogeneous formations (σ_Y^2 = 16). Recently, many studies have focused on developing the spatial correlation structure in the multimodal [231] and hierarchical multimodal frameworks [8] because it is more realistic when the correlation scale is neither single nor finite valued [2]. Deng et al. [232] extended the effective retardation developed by Rajaram [229] to hierarchical multimodal media. Based on their results, Soltanian et al. [233] formulated the reactive macrodispersivity within a hierarchical multimodal framework. The hierarchical multimodal Lagrangian-based transport model can incorporate the physical properties of the formation, such as volume proportion or mean length, to estimate the transport parameters [234]. Since geological data is much more abundant than permeability measurements, a more accurate spatial correlation structure of permeability can be obtained [207]. Also, since the Lagrangian framework is suitable for stable numerical computation, the Lagrangian numerical method also avoids the traditional global assumptions of the analytical method [235]. In the Lagrangian numerical framework, the assumptions are local (within the scale of computational grids), making it an effective tool to bridge the gap between lab-scale measurements and field-scale estimates of transport parameters.

The Lagrangian particle-tracking and reaction method is a generated Lagrangian method that has been successfully used to quantify chemical heterogeneity in diffusion-controlled bimolecular reactions [236]. It is further extended to upscale Monod-type reactions in realistic field bioremediation experiments from column or batch scale experiments [237]. The gap between theory and practice that was proposed can be partially closed if user-friendly stochastic subsurface hydrology toolkits are developed [238,239]. Over the years, some toolkits have been programmed and tried to be extended to communities [240,241]. But the efficiency produced seems not quite evident and the applications are still on the way.

5.2. Stochastic fractals

The fractal geometry method deals mainly with the distribution of the media's intrinsic characterizations or structure, such as pore properties. To expand the application of fractal theory to dynamic flow and transport processes in heterogeneous aquifers, time-series and spatial variations have been considered in the fractal with time as the independent variable. Fractional Brownian motion (FBM) is a common statistical model that parsimoniously explains the expansion of

heterogeneity at all scales. Other correlation models include, but are not limited to, fractal dimensions, fractional Brownian noise, fractal trajectories, Hurst coefficient models, Taylor random walks, and fractional Levy motions [242]. Using the concept of scale constancy, these models are capable of quantifying heterogeneous hydraulic properties in both space and time.

Considering FBM as an example of a commonly used fractal model of heterogeneity, the FBM $B_H(t)$ is a statistically self-similar Gaussian process with respect to the Hurst exponent H ($0 < H < 1$), which decays as a power law [243]. The FBM is defined through its increments $W_H(t,s) = B_H(t)\text{-}B_H(s)$, which are normally distributed with $N(0,(t\text{-}s)^{2H})$ but not independent. A one-dimensional FBM that passes through the origin (i.e., $B_H(0) = 0$ at $t = 0$) can be expressed as the difference between the original notation of FBM and the value of the random function at $t = 0$ [244].

$$B_H(t) = \frac{1}{\Gamma(H+0.5)}\left(\int_{-\infty}^{0}\left[(t-s)^{H-1/2} - (-s)^{H-1/2}\right]\right)dB(s) + \int_0^t (s-H)^{H-1/2}dB(s) \tag{5.10}$$

where Γ is the Gamma function and $B(s)$ represents a Brownian process that possesses zero mean and unit variance. The exponent H controls the correlation of the FBM function, and its value dictates the diffusion type manifested by the FBM process. The expression $0 < H < 1/2$ corresponds to a negative correlation zone, which represents a subdiffusive or antipersistent behavior. The value $H = 1/2$ indicates zero correlation, and represents a unique instance of Gaussian noise, random walk, or increments of Brownian motion, which models Fickian diffusion. Positive correlation is given by $1/2 < H < 1$, where the FBM models superdiffusion, or persistent behavior [245].

$$\mathbf{E}[B_H(t)B_H(s)] = \frac{1}{2}\left\{t^{2H} + s^{2H} - (t-s)^{2H}\right\} \tag{5.11}$$

$$\langle x^2(t)\rangle = \boldsymbol{E}\left[B_H^2(t)\right] = t^{2H} \tag{5.12}$$

The applications of FBM are broad. By assuming that the semivariogram of log hydraulic conductivity fluctuation is fractal, Neuman [38] developed a so-called "universal" scaling rule to upscale hydraulic conductivity and dispersivity. The derived upscaling equation can be applied to a wide range of scales and a broad class of geological media. The method can characterize one property as a single fractal geometry or may be extended to characterize the distribution of hydraulic conductivity with varied fractal dimensions in a multi-fractal system [246]. The work indicated that the variation of K is different from the characteristics of monofractals, which are more heterogeneous at smaller scales than larger scales.

For its application in Fickian-type diffusion, a time-dependent diffusion coefficient $D(t)$ can be derived with the constant fractal diffusion coefficient D_H, $D(t) = 2HD_H t^{2H-1}$. Zhokh and Strizhak [247] developed a model to mimic the non-Fickian growth observed in field site plumes based on the fractal-like dispersive behavior of dispersing particles transported through subsurface porous media. Zhokh and Strizhak [248] developed and compared diffusion scaling equations based on time-fractional diffusion, the standard diffusion, and the FBM in a porous pellet, respectively, and found no significant discrepancies among the results.

Rather than use the correlation of hydraulic conductivity, Nduny and Addison [249] extended the FBM to generate scale-dependent dispersion by assuming that the movement of water and dispersing solute particles are self-affine fractals. Agboola et al. [250] showed that the surface and volume of adsorbent particles might also have scale-invariant properties, and thus fractal behavior may be considered in the sorption process. The fractal description may also predict the reaction rate by assuming that reaction rates are scale-dependent, as given in basalt weathering at a given length scale from BET scale reaction rate [251]. Groundwater flow and transport through various media can also be represented through the adaptation of the fractal concept. Lu et al. [252] developed a novel, fractional derivative of the advection–dispersion-reaction equation to simulate the first-order decay of nitrate in porous media. Concurrently, Nikan et al. [252] efficiently solved the fractal mobile-immobile transport model using a technique based on radial basis function-generated finite difference.

5.3. Strengths and limitations of analytical and numerical solutions

The attractiveness of the analytic method resides in its simplicity of using statistical characteristics to represent properties of a whole formation. However, it is restricted by assumptions made that are needed to gain the well-posedness (closure) of the stochastic equations (see a discussion by Wood et al. [204]). The restrictive global assumptions are required because they are based on analytical tools such as Fourier analysis. Common assumptions include:

(1) Ergodicity. This means a single scale of spatial correlation, or, at the other extreme, a continuous (fractal) correlation scale exists with a critical correlation range [253]. Meanwhile, the scale of plume motion is long compared to spatial correlation scales of heterogeneity. Therefore, in layered sediments or strata, the method is not quite effective;
(2) Statistical stationarity. A lognormal or bi-variate distributed conductivity field that allows its entire probability density function is described with the first two moments;
(3) The results are mostly valid for small variances where $\sigma_Y^2 < 1$ in spatial heterogeneity though some stochastic methods can be applied to relatively high values. The effective parameters could be greatly underestimated in high heterogeneous media;
(4) Infinite or unbounded domain extent. This guarantees to produce the covariance or variogram between head/concentration and conductivity/transmissivity. The assumption is acceptable at distances far from the no-flow or constant boundaries, but not feasible for complex boundaries.

In practice, the stochastic models are occasionally used in the modeling of tracer propagation in natural subsurfaces and laboratory columns and fit experimental data well. But as the above assumptions are in contradiction with the experiment settings, the results are not accurate enough to explain how the solute dispersion is affected by porous matrix structure or its sorptive properties. At last, detailed sedimentary statistical architecture data is always required to provide accurate quantification of spatial correlation structures [207]. In application, the data is often obtained through geophysical methods not easy, especially for high spatial resolution data. That is the reason why the field tests of such methods are only conducted in several sites, including Espanola Basin, New Mexico [254], and Borden site, Canada [255]. The extent to which the resolution of sedimentary architecture data affects the prediction accuracy was discussed in Dai et al. [207].

Besides characterizing the random parameter field with moments, we can obtain the full distribution directly with the numerical frameworks. The numerical approach deploys Monte Carlo methods, Bayesian

and other conditioning methods, to simulate a large amount of realizations to represent the uncertainties of the formation with geostatistically valid results [256]. The Monte Carlo methods may analyze the ensemble statistics of the head and concentration fields or solve the moment equations themselves [257]. The strength of the numerical method lies in its robustness in representing formation heterogeneities. The development of computing ability and capacity further extends its applications.

5.4. Implementation of stochastic methods

With the extensive achievements and "stochastic revolution" over the past 20 years, an enormous number of theoretical publications have been produced. However, practical applications of stochastic methods in the hydrological community to aquifer management still largely fall behind. Reasons for why there has been a low impact of stochastic subsurface hydrology on practice have been explored by Cirpka and Valocchi [258]. Efforts for commonly blamed shortcomings such as developing computational tools and training have been gradually made to minimize the gap between theories and applications and encourage the hydrologists to apply it regularly to aquifer modeling and management. Liu et al. [259] developed a code MODFLOW-STO that attached the stochastic analysis to widely used codes MODFLOW-2000. Unfortunately, as it needs large field-site data, a multidisciplinary effort involving geostatistical, stochastic, and involvement of numerical modelers, and real-world applications are still limited.

In contrast, the analysis based on the concept of Monte Carlo analysis associated with the uncertainty analysis in groundwater management is widely adopted both in academia and industry. This partly benefits from the rich software or codes for sampling, and their flexibility of coupling with the modeling software partly benefits from the rapid development of computational capacity, which greatly reduces the cost for numerous model runs.

6. Summary and future prospects

With the understanding of the physical and chemical properties of subsurface systems, large-scale accurate estimations of effective parameters are needed for characterizing subsurface processes across different spatial scales. Significant and up-to-date approaches of upscaling flow and transport processes from lab to field scales are reviewed. There is certainly no universal agreement on which method is superior to the others. Different schemes/algorithms display varying degrees of rigor and sophistication. The comparisons of the various methods are quite rare in a general framework. Various points exist when considering the difficulty of acquiring porous media property distributions and the assumptions needed to perform valid analyses. Therefore, the choice of an appropriate method is always case-dependent.

First, it is needed to characterize and identify the flow and transport mechanisms and the parameters involved in the model being addressed. Definitely, more choices are provided for upscaling conductivity or dispersivity than reactive geochemical parameters. The implementation of upscaling processes is relatively simpler for flow processes than for transport and reaction processes. If we intend to upscale reaction rates, the asymptotic and volume averaging methods are preferred. Therefore, the derivation of governing equations in field scale is inevitable.

Second, the heterogeneity level and distribution properties do affect the choice of upscaling methods. If the formation heterogeneity is high with a large log permeability variance, the general stochastic method may not be applicable. But, in practice, the related requirements such as stationarity, ergodicity, mean uniform flow, and Gaussian distribution could often be substantially relaxed. A comparison can be conducted to check how the results deviated from the observations and whether they can be accepted for practical purposes. Wavelet analysis is a good choice for highly heterogeneous formations, especially when the hydraulic conductivity distribution has a wide range. If non-Fickian transport is obvious in the heterogeneous formation, the upscaled equations are better to capture the long-lasting solute transport tail.

Third, the upgridding levels that the model supposes to be coarsened play a role in the model selection. The physically-based methods are favorable to highly disordered porous media, but so far, very few field application cases have been published yet. On the other hand, the fractal and machine learning methods have been extensively applied for pore-scale flow and transport problems such as porous structure characterization and permeability scaling.

Forth, the quality and quantity of available data play an important role in the upscaling method selection. As discussed above, the conventional standard field data are often too limited to provide sufficient geostatistical measurements needed for upscaling flow and transport parameters with stochastic methods. Solving the stochastic equations with time- or space-dependent parameters is an option to establish directly the quantitative relationship between the laboratory- and field-scale parameters. The target observations like hydraulic heads or concentrations are as well important for model calibration in the scale of interest. The lack of structure information of the subsurface formations sometimes can be compensated with large observations with parameter prior information or scenario analysis under a Monte Carlo scheme.

In addition, an open question has been raised about if one can make so-called "deterministic" predictions in the modeling process, especially when considering the uncertainty or chaos generated in the upscaling process. Though limitations in the specific method often motivate many investigators to revert and employ conventional advection–dispersion equation approaches in practice for considering the natural heterogeneity, it can be marked that the simulations are intrinsically uncertain due to current economic and technical limitations. Instead of obtaining a perfectly accurate solution of a single realization that is likely not represented by real-world properties, probabilistic results with uncertainty quantification offer a new perspective to capture and characterize the subsurface heterogeneity. With the development of newer uncertainty quantification algorithms based on deep learning and big data techniques, future subsurface characterizations would obtain more powerful computation resources and reliable parameter upscaling results.

Although substantial advances have been achieved on upscaling method development in recent decades, there are still a couple of drawbacks or difficulties affecting the application of the upscaling methods. One of the most serious drawbacks or bottlenecks is the lack of sufficient multi-scale geological data for applying the upscaling algorithms. New geophysical measurement technologies such as electrical resistivity, ground-penetrating radar, and passive seismic imaging all have potential in big data acquirement for subsurface characterization with much better resolutions. The artificial intelligence originated methods applied in geology with a big database would inspire more geophysical projects for property measurements at different scales.

Another drawback is that though many analytical and numerical upscaling studies have been published, only a small number of field case applications are available for strictly validating these upscaling algorithms. Without enough large-scale field observations for verification, it is hard to judge whether an upscaled parameter provides a good or bad prediction. It is worth conducting more field-scale transport experiments to verify the effectiveness and applicability of upscaling techniques and upscaled parameters.

In conclusion, this study provides valuable insights for a better understanding of multiscale subsurface systems. With this review, people who are not familiar with upscaling concepts can have an initial understanding of subsurface scaling issues and start to apply upscaling techniques for solving practical geological and energy problems. Besides the upscaling methods described in this paper, approaches such as multiscale finite element methods, non-local multi-continuum method, and other methods that directly deal with upscaling are increasingly applied in the flow and transport processes. Although upscaling approaches have been studied for a few decades, they are generally

abstract, complex, and difficult to implement even for scientists who developed them. Currently, upscaling accuracy, flexibility, efficiency, and robustness need further verification and justification. These challenges provide great motivation for continued research into upscaling algorithms for effectively addressing fluid flow and transport processes in heterogeneous media. A generic integrated upscaling framework is needed to incorporate the current upscaling algorithms, uncertainty quantification techniques, data sciences, and artificial intelligence for further investigation to bridge the gap between upscaling algorithms and real-world applications for energy and environmental engineering in the future.

Declaration of Competing Interest

The authors declare that they have no known competing financial interests or personal relationships that could have appeared to influence the work reported in this paper.

Acknowledgements

This work was jointly supported by the National Key Research and Development Program of China (No. 2018YFC1800900), National Natural Science Foundation of China (No: 41972249, 41772253, 51774136), the Program for Jilin University (JLU) Science and Technology Innovative Research Team (No. 2019TD-35), Graduate Innovation Fund of Jilin University (No: 101832020CX240), Natural Science Foundation of Hebei Province of China (D2017508099), and the Program of Education Department of Hebei Province (QN219320). Additional funding was provided by the Engineering Research Center of Geothermal Resources Development Technology and Equipment, Ministry of Education, China.

References

[1] Gómez-Hernández JJ, Butler JJ, Fiori A, Bolster D, Cvetkovic V, Dagan G, et al. Introduction to special section on Modeling highly heterogeneous aquifers: Lessons learned in the last 30 years from the MADE experiments and others. Water Resour Res 2017;53(4):2581–4.
[2] Soltanian MR, Ritzi RW. A new method for analysis of variance of the hydraulic and reactive attributes of aquifers as linked to hierarchical and multiscaled sedimentary architecture. Water Resour Res 2014;50(12):9766–76.
[3] Rangriz Shokri A, Babadagli T. Feasibility assessment of heavy-oil recovery by CO2 injection after cold production with sands: Lab-to-field scale modeling considering non-equilibrium foamy oil behavior. Appl Energy 2017;205:615–25.
[4] Zachara J, Brantley S, Chorover J, Ewing R, Kerisit S, Liu C, et al. Internal domains of natural porous media revealed: critical locations for transport, storage, and chemical reaction. Environ Sci Technol 2016;50(6):2811–29.
[5] Klaver J, Desbois G, Urai JL, Littke R. BIB-SEM study of the pore space morphology in early mature Posidonia Shale from the Hils area, Germany. Int. J. Coal Geol. 2012;103:12–25.
[6] Ross DJK, Marc Bustin R. The importance of shale composition and pore structure upon gas storage potential of shale gas reservoirs. Mar Pet Geol 2009;26(6):916–27.
[7] Saif T, Lin Q, Butcher AR, Bijeljic B, Blunt MJ. Multi-scale multi-dimensional microstructure imaging of oil shale pyrolysis using X-ray micro-tomography, automated ultra-high resolution SEM, MAPS Mineralogy and FIB-SEM. Appl. Energy 2017;202:628–47.
[8] Dai Z, Zhang Ye, Bielicki J, Amooie MA, Zhang M, Yang C, et al. Heterogeneity-assisted carbon dioxide storage in marine sediments. Appl Energy 2018;225:876–83.
[9] Yang C, Wang T, Li Y, Yang H, Li J, Qu D, et al. Feasibility analysis of using abandoned salt caverns for large-scale underground energy storage in China. Appl Energy 2015;137:467–81.
[10] Xu C, Dowd PA, Tian ZF. A simplified coupled hydro-thermal model for enhanced geothermal systems. Appl Energy 2015;140:135–45.
[11] Loschko M, Wöhling T, Rudolph DL, Cirpka OA. An electron-balance based approach to predict the decreasing denitrification potential of an aquifer. Groundwater 2019;57(6):925–39.
[12] Hartmann A. Putting the cat in the box: why our models should consider subsurface heterogeneity at all scales. Wiley Interdiscip. Rev. Water 2016;3(4):478–86.
[13] Dai Z, Viswanathan H, Middleton R, Pan F, Ampomah W, Yang C, et al. CO2 accounting and risk analysis for CO2 sequestration at enhanced oil recovery sites. Environ Sci Technol 2016;50(14):7546–54.
[14] Yang C, Dai Z, Romanak KD, Hovorka SD, Treviño RH. Inverse modeling of water-rock-CO2 batch experiments: Potential impacts on groundwater resources at carbon sequestration sites. Environ Sci Technol 2014;48(5):2798–806.
[15] Jia W, Pan F, Dai Z, Xiao T, McPherson B. Probabilistic risk assessment of CO2 trapping mechanisms in a sandstone CO2-EOR field in northern texas, USA. Energy Procedia 2017;114:4321–9.
[16] Willmann M, Carrera J, Sánchez-Vila X. Transport upscaling in heterogeneous aquifers: What physical parameters control memory functions? Water Resour Res 2008;44(12):177–85.
[17] Rovey CW. The scaling properties of geological media with respect to groundwater flow and transport. Groundwater: Prentice-Hall; 2009.
[18] Zech A, Attinger S, Cvetkovic V, Dagan G, Dietrich P, Fiori A, et al. Is unique scaling of aquifer macrodispersivity supported by field data? Water Resour Res 2015;51(9):7662–79.
[19] Kuntz BW, Rubin S, Berkowitz B, Singha K. Quantifying Solute Transport at the Shale Hills Critical Zone Observatory. Vadose Zone J 2011;10(3):843–57.
[20] Fiori A, Bellin A, Cvetkovic V, de Barros FPJ, Dagan G. Stochastic modeling of solute transport in aquifers: From heterogeneity characterization to risk analysis. Water Resour Res 2015;51(8):6622–48.
[21] Dentz M, Scher H, Holder D, Berkowitz B. Transport behavior of coupled continuous-time random walks. Phys Rev E: Stat Nonlinear Soft Matter Phys 2008;78(4):041110.
[22] Durlofsky LJ. Numerical calculation of equivalent grid block permeability tensors for heterogeneous porous media. Water Resour Res 1991;27(5):699–708.
[23] Sahimi M. Flow and transport in porous media and fractured rock: from classical methods to modern approaches. John Wiley & Sons; 2011.
[24] Soltanian MR, Dai Z, Yang C, Amooie MA, Moortgat J. Multicomponent competitive monovalent cation exchange in hierarchical porous media with multimodal reactive mineral facies. Stoch Env Res Risk Assess 2018;32(1):295–310.
[25] Soltanian MR, Ritzi RW, Huang CC, Dai Z. Relating reactive solute transport to hierarchical and multiscale sedimentary architecture in a L agrangian-based transport model: 1. Time-dependent effective retardation factor. Water Resour Res 2015;51(3):1586–600.
[26] Rubin Y. Applied stochastic hydrogeology. New York: Oxford University Press; 2003.
[27] Neuman SP, Tartakovsky DM. Perspective on theories of non-Fickian transport in heterogeneous media. Adv Water Resour 2009;32(5):670–80.
[28] Wang H, Chen Li, Qu Z, Yin Y, Kang Q, Yu Bo, et al. Modeling of multi-scale transport phenomena in shale gas production—a critical review. Appl Energy 2020;262:114575. https://doi.org/10.1016/j.apenergy.2020.114575.
[29] Zhang K, Jia Na, Li S, Liu L. Static and dynamic behavior of CO2 enhanced oil recovery in shale reservoirs: Experimental nanofluidics and theoretical models with dual-scale nanopores. Appl Energy 2019;255:113752. https://doi.org/10.1016/j.apenergy.2019.113752.
[30] Wolfsberg A, Dai Z, Zhu L, Reimus P, Xiao T, Ware D. Colloid-facilitated plutonium transport in fractured tuffaceous rock. Environ Sci Technol 2017;51(10):5582–90.
[31] Dai Z, Xu L, Xiao T, McPherson B, Zhang X, Zheng L, et al. Reactive chemical transport simulations of geologic carbon sequestration: Methods and applications. Earth Sci Rev 2020;103265.
[32] Pan F, McPherson BJ, Dai Z, Jia W, Lee S-Y, Ampomah W, et al. Uncertainty analysis of carbon sequestration in an active CO2-EOR field. Int J Greenhouse Gas Control 2016;51:18–28.
[33] Bierkens MFP, Van der Gaast JWJ. Upscaling hydraulic conductivity: theory and examples from geohydrological studies. Nutr Cycl Agroecosyst 1998;50(1–3):193–207.
[34] Foroughi S, Jamshidi S, Masihi M. Lattice Boltzmann method on quadtree grids for simulating fluid flow through porous media: a new automatic algorithm. Phys A 2013;392(20):4772–86.
[35] Dagan G. Flow and transport in porous formations. New York: Springer; 1989.
[36] Kitanidis PK. Persistent questions of heterogeneity, uncertainty, and scale in subsurface flow and transport. Water Resour Res 2015;51(8):5888–904.
[37] Hassan AE, Cushman JH, Delleur JW. Monte Carlo studies of flow and transport in fractal conductivity fields: Comparison with stochastic perturbation theory. Water Resour Res 1997;33(11):2519–34.
[38] Neuman SP. Universal scaling of hydraulic conductivities and dispersivities in geologic media. Water Resour Res 1990;26(8):1749–58.
[39] Hunt AG, Sahimi M. Flow, transport, and reaction in porous media: Percolation scaling, critical-path analysis, and effective medium approximation. Rev Geophys 2017;55(4):993–1078.
[40] Farmer CL. Upscaling: A review. Int J Numer Meth Fluids 2002;40(1–2):63–78.
[41] Miller AW, Rodriguez DR, Honeyman BD. Upscaling sorption/desorption processes in reactive transport models to describe metal/radionuclide transport: A critical review. Environ Sci Technol 2010;44(21):7996–8007.
[42] Bear J. Hydraulics of groundwater. New York: Mc GrawHill Inc; 1979.
[43] Benson DA, Wheatcraft SW, Meerschaert MM. The fractional-order governing equation of Lévy Motion. Water Resour Res 2000;36(6):1413–23.
[44] Chapuis RP, Dallaire V, Marcotte D, Chouteau M, Acevedo N, Gagnon F. Evaluating the hydraulic conductivity at three different scales within an unconfined sand aquifer at Lachenaie, Quebec. Can. Geotech. J. 2005;42(4):1212–20.
[45] Azizmohammadi S, Matthäi SK. Is the permeability of naturally fractured rocks scale dependent? Water Resour Res 2017;53(9):8041–63.

[46] Pedretti D, Russian A, Sanchez-Vila X, Dentz M. Scale dependence of the hydraulic properties of a fractured aquifer estimated using transfer functions. Water Resour Res 2016;52(7):5008–24.
[47] Godoy VA, Zuquette LV, Gómez-Hernández JJ. Scale effect on hydraulic conductivity and solute transport: Small and large-scale laboratory experiments and field experiments. Eng Geol 2018;243:196–205.
[48] Schulze-Makuch D, Cherkauer DS. Facies dependent scale behaviour of hydraulic conductivity and longitudinal dispersivity. IAHS Publ-Ser Proc Rep-Intern Assoc Hydrol Sci 1995;225:157–64.
[49] Clauser C. Permeability of crystalline rocks. Eos Trans Am Geophys Union 1992; 73(21).
[50] Nastev M, Savard MM, Lapcevic P, Lefebvre R, Martel R. Hydraulic properties and scale effects investigation in regional rock aquifers, south-western Quebec, Canada. Hydrogeol J 2004;12(3):257–69.
[51] Schulze-Makuch D, Carlson DA, Cherkauer DS, Malik P. Scale Dependency of Hydraulic Conductivity in Heterogeneous Media. Ground Water 1999;37(6): 904–19.
[52] Schulze-Makuch D, Cherkauer DS. Variations in hydraulic conductivity with scale of measurement during aquifer tests in heterogeneous, porous carbonate rocks. Hydrogeol J 1998;6(2):204–15.
[53] Dagan G. Solute transport in heterogeneous porous formation. J Fluid Mech 1984; 145(-1):151–77.
[54] Appelo CAJ, Postma D. Geochemistry, groundwater and pollution. 2nd. Ed. Rotterdam: Balkema; 2005.
[55] Klotz D, Seiler KP, Moser H, Neumaier F. Dispersivity and velocity relationship from laboratory and field experiments. J Hydrol 1980;45(3–4):169–84.
[56] Abgaze TA, Sharma PK. Solute transport through porous media with scale-dependent dispersion and variable mass transfer coefficient. ISH J Hydr Eng 2015;21(3):298–311.
[57] Hauns M, Jeannin PY, Atteia O. Dispersion, retardation and scale effect in tracer breakthrough curves in karst conduits. J Hydrol 2001;241(3–4):177–93.
[58] Berkowitz B, Dror I, Hansen SK, Scher H. Measurements and models of reactive transport in geological media. Rev Geophys 2016;54(4):930–86.
[59] Krantz WB. Scaling analysis in modeling transport and reaction processes: A systematic approach to model building and the art of approximation. London: John Wiley & Sons; 2007.
[60] Gelhar LW, Welty C, Rehfeldt KR. A critical review of data on field-scale dispersion in aquifers. Water Resour Res 1992;28(7):1955–74.
[61] Schulze-Makuch D. Longitudinal dispersivity data and implications for scaling behavior. Groundwater 2005;43(3):443–56.
[62] Rolle M, Chiogna G, Hochstetler DL, Kitanidis PK. On the importance of diffusion and compound-specific mixing for groundwater transport: An investigation from pore to field scale. J Contam Hydrol 2013;153:51–68.
[63] Churakov SV, Gimmi T. Up-scaling of molecular diffusion coefficients in clays: A two-step approach. J Phys Chem C 2011;115(14):6703–14.
[64] Dai Z, Wolfsberg A, Lu Z, Ritzi RW. Representing aquifer architecture in macrodispersivity models with an analytical solution of the transition probability matrix. Geophys Res Lett 2007;34(20).
[65] Reimus PW, Callahan TJ. Matrix diffusion rates in fractured volcanic rocks at the Nevada Test Site: Evidence for a dominant influence of effective fracture apertures. Water Resour Res 2007;43:W07421.
[66] Liu HH, Bodvarsson GS, Zhang G. Scale dependency of the effective matrix diffusion coefficient. Vadose Zone J 2004;3(1):312–5.
[67] Neretnieks I. A stochastic multi-channel model for solute transport—analysis of tracer tests in fractured rock. J Contam Hydrol 2002;55(3–4):175–211.
[68] Liu H, Zhang Y, Molz FJ. Scale dependence of the effective matrix diffusion coefficient: Evidence and preliminary interpretation. Lawrence Berkeley National Laboratory; 2006.
[69] Zhou Q, Liu H, Molz FJ, Zhang Y, Bodvarsson GS. Field-scale effective matrix diffusion coefficient for fractured rock: Results from literature survey. J Contam Hydrol 2007;93(1–4):161–87.
[70] Deng H, Molins S, Trebotich D, Steefel C, DePaolo D. Pore-scale numerical investigation of the impacts of surface roughness: Upscaling of reaction rates in rough fractures. Geochim Cosmochim Acta 2018;239:374–89.
[71] Brusseau ML, Chorover J. Chemical processes affecting contaminant transport and fate. In: Environmental and Pollution Science. Academic Press; 2019. p. 113–30.
[72] Limousin G, Gaudet J-P, Charlet L, Szenknect S, Barthès V, Krimissa M. Sorption isotherms: A review on physical bases, modeling and measurement. Appl Geochem 2007;22(2):249–75.
[73] Freeze RA, Cherry JA. Groundwater. New Jersey: Prentice-Hall; 1979.
[74] Zhang X, Liu C, Hu BX, Zhang G. Uncertainty analysis of multi-rate kinetics of uranium desorption from sediments. J Contam Hydrol 2014;156:1–15.
[75] Springob G, Böttcher J. Parameterization and regionalization of Cd sorption characteristics of sandy soils. II. Regionalization: Freundlich k estimates by pedotransfer functions. J Plant Nutr Soil Sci 1998;161(6):689–96.
[76] Dai Z, Zhan C, Soltanian MR, Ritzi RW, Zhang X. Identifying spatial correlation structure of multimodal permeability in hierarchical media with Markov chain approach. J Hydrol 2019;568:703–15.
[77] Maghrebi M, Jankovic I, Fiori A, Dagan G. Effective retardation factor for transport of reactive solutes in highly heterogeneous porous formations. Water Resour Res 2013;49(12):8600–4.
[78] Fernández-Garcia D, Illangasekare TH, Rajaram H. Differences in the scale dependence of dispersivity and retardation factors estimated from forced-gradient and uniform flow tracer tests in three-dimensional physically and chemically heterogeneous porous media. Water Resour Res 2005;41:W03012.
[79] Giammar DE, Hering JG. Time scales for sorption− desorption and surface precipitation of uranyl on goethite. Environ Sci Technol 2001;35(16):3332–7.
[80] Zhang X, Liu C, Hu BX, Hu Q. Grain-Size Based Additivity Models for Scaling Multi-rate Uranyl Surface Complexation in Subsurface Sediments. Math Geosci 2016;48(5):511–35.
[81] Maher K, Chamberlain CP. Hydrologic regulation of chemical weathering and the geologic carbon cycle. Science 2014;343(6178):1502–4.
[82] De Windt L, Pellegrini D, Van Der Lee J. Coupled modeling of cement/claystone interactions and radionuclide migration. J Contam Hydrol 2004;68(3–4):165–82.
[83] Sverdrup H. Chemical weathering of soil minerals and the role of biological processes. Fungal Biology Reviews 2009;23(4):94–100.
[84] Ruiz-Agudo E, Putnis CV, Putnis A. Coupled dissolution and precipitation at mineral–fluid interfaces. Chem Geol 2014;383:132–46.
[85] Morse JW, Arvidson RS. The dissolution kinetics of major sedimentary carbonate minerals. Earth Sci Rev 2002;58(1–2):51–84.
[86] Vriens B, Seigneur N, Mayer KU, Beckie RD. Scale dependence of effective geochemical rates in weathering mine waste rock. J Contam Hydrol 2020;234: 103699. https://doi.org/10.1016/j.jconhyd.2020.103699.
[87] Chou L, Garrels RM, Wollast R. Comparative study of the kinetics and mechanisms of dissolution of carbonate minerals. Chem Geol 1989;78(3–4): 269–82.
[88] White AF, Schulz MS, Lawrence CR, Vivit DV, Stonestrom DA. Long-term flow-through column experiments and their relevance to natural granitoid weathering rates. Geochim Cosmochim Acta 2017;202:190–214.
[89] Jung H, Navarre-Sitchler A. Scale effect on the time dependence of mineral dissolution rates in physically heterogeneous porous media. Geochim Cosmochim Acta 2018;234:70–83.
[90] Moore J, Lichtner PC, White AF, Brantley SL. Using a reactive transport model to elucidate differences between laboratory and field dissolution rates in regolith. Geochim Cosmochim Acta 2012;93:235–61.
[91] Levenson Y, Ryb U, Emmanuel S. Comparison of field and laboratory weathering rates in carbonate rocks from an eastern mediterranean drainage basin. Earth Planet Sci Lett 2017;465:176–83.
[92] White A, Blum A, Schulz M, Bullen T, Harden J, Peterson M. Chemical weathering of a soil chronosequence on granitic alluvium: 1. Reaction rates based on changes in soil mineralogy. Geochim Cosmochim Acta 1996;60:2533–50.
[93] Salehikhoo F, Li Li, Brantley SL. Magnesite dissolution rates at different spatial scales: The role of mineral spatial distribution and flow velocity. Geochim Cosmochim Acta 2013;108:91–106.
[94] Li Li, Steefel CI, Yang Li. Scale dependence of mineral dissolution rates within single pores and fractures. Geochim Cosmochim Acta 2008;72(2):360–77.
[95] Jia W, Xiao T, Wu Z, Dai Z, McPherson B. Impact of Mineral Reactive Surface Area on Forecasting Geological Carbon Sequestration in a CO2-EOR Field. Energies 2021;14(6):1608.
[96] Qin C-Z, Hassanizadeh SM, Ebigbo A. Pore-scale network modeling of microbially induced calcium carbonate precipitation: Insight into scale dependence of biogeochemical reaction rates. Water Resour Res 2016;52(11):8794–810.
[97] Hodson ME, Langan SJ, Kennedy FM, Bain DC. Variation in soil surface area in a chronosequence of soils from Glen Feshie, Scotland and its implications for mineral weathering rate calculations. Geoderma 1998;85(1):1–18.
[98] Stolze L, Zhang Di, Guo H, Rolle M. Model-based interpretation of groundwater arsenic mobility during in situ reductive transformation of ferrihydrite. Environ Sci Technol 2019;53(12):6845–54.
[99] Meile C, Scheibe TD. Reactive transport modeling of microbial dynamics. Elements 2019;15(2):111–6.
[100] Barajas-Rodriguez FJ, Murdoch LC, Falta RW, Freedman DL. Simulation of in situ biodegradation of 1,4-dioxane under metabolic and cometabolic conditions. J Contam Hydrol 2019;223:103464. https://doi.org/10.1016/j.jconhyd.2019.02.006.
[101] Giannetta MG, Sanford RA, Druhan JL. A modified Monod rate law for predicting variable S isotope fractionation as a function of sulfate reduction rate. Geochim Cosmochim Acta 2019;258:174–94.
[102] Chezeau B, Vial C. Modeling and simulation of the biohydrogen production processes. Biohydrogen: Elsevier; 2019. p. 445–83.
[103] Sun Y, Petersen JN, Clement TP, Hooker BS. Effect of reaction kinetics on predicted concentration profiles during subsurface bioremediation. J Contam Hydrol 1998;31(3–4):359–72.
[104] Ding D, Benson DA. Simulating biodegradation under mixing-limited conditions using Michaelis-Menten (Monod) kinetic expressions in a particle tracking model. Adv Water Resour 2015;76:109–19.
[105] Sturman PJ, Stewart PS, Cunningham AB, Bouwer EJ, Wolfram JH. Engineering scale-up of in situ bioremediation processes: A review. J Contam Hydrol 1995;19 (3):171–203.
[106] Zhang X, Hu BX, Ren H, Zhang J. Composition and functional diversity of microbial community across a mangrove-inhabited mudflat as revealed by 16S rDNA gene sequences. Sci Total Environ 2018;633:518–28.
[107] Chen L, Hu BX, Dai H, Zhang X, Xia C-A, Zhang J. Characterizing microbial diversity and community composition of groundwater in a salt-freshwater transition zone. Sci Total Environ 2019;678:574–84.
[108] Lu Z, Wolfsberg AV, Dai Z, Zheng C. Characteristics and controlling factors of dispersion in bounded heterogeneous porous media. Water Resour Res 2010;46: W12508.
[109] Sim Y, Chrysikopoulos CV. Analytical models for one-dimensional virus transport in saturated porous media. Water Resour Res 1995;31(5):1429–37.
[110] De Barros FP, Rubin Y. Modelling of block-scale macrodispersion as a random function. J Fluid Mech 2011;676:514.

[111] Journel AG. Geostatistics: models and tools for the earth sciences. Math Geol 1986;18(1):119–40.
[112] Dagan G, Rabinovich A. Oscillatory pumping wells in phreatic, compressible, and homogeneous aquifers. Water Resour Res 2014;50(8):7058–66.
[113] Durlofsky LJ. Representation of grid block permeability in coarse scale models of randomly heterogeneous porous media. Water Resour Res 1992;28(7):1791–800.
[114] Rubin Y, Gómez-Hernández JJ. A stochastic approach to the problem of upscaling of conductivity in disordered media: Theory and unconditional numerical simulations. Water Resour Res 1990;26(4):691–701.
[115] Hristopulos DT. Renormalization group methods in subsurface hydrology: overview and applications in hydraulic conductivity upscaling. Adv Water Resour 2003;26(12):1279–308.
[116] Vermeulen PTM, Stroet CBMT, Heemink AW. Limitations to upscaling of groundwater flow models dominated by surface water interaction. Water Resour Res 2006;42(10).
[117] Dagan G, Fiori A, Jankovic I. Upscaling of flow in heterogeneous porous formations: Critical examination and issues of principle. Adv Water Resour 2013;51:67–85.
[118] Duquerroix J, Lemouzy P, Noetinger B, Romeu R. Influence of the permeability anisotropy ratio on large-scale properties of heterogeneous reservoirs. SPE Annual Technical Conference and Exhibition: OnePetro. 1993.
[119] Scheibe T, Yabusaki S. Scaling of flow and transport behavior in heterogeneous groundwater systems. Adv Water Resour 1998;22(3):223–38.
[120] Ghanbarian B, Hunt AG. Fractals: concepts and applications in geosciences. Florida: CRC Press; 2017.
[121] Guéguen Y, Le Ravalec M, Ricard L. Upscaling: effective medium theory, numerical methods and the fractal dream. Pure Appl Geophys 2006;163(5–6):1175–92.
[122] Xu P, Li C, Qiu S, Sasmito AP. A fractal network model for fractured porous media. Fractals 2016;24(02):1650018.
[123] Mandelbrot BB. The fractal geometry of nature. New York: Freeman; 1983.
[124] Molz FJ, Rajaram H, Lu S. Stochastic fractal-based models of heterogeneity in subsurface hydrology: Origins, applications, limitations, and future research questions. Rev Geophys 2004;42(1).
[125] Velde B, Dubois J, Moore D, Touchard G. Fractal patterns of fractures in granites. Earth Planet Sci Lett 1991;104(1):25–35.
[126] Yu Xu, Regenauer-Lieb K, Tian F-B. Effects of surface roughness and derivation of scaling laws on gas transport in coal using a fractal-based lattice Boltzmann method. Fuel 2020;259:116229. https://doi.org/10.1016/j.fuel.2019.116229.
[127] Gimenez D, Perfect E, Rawls WJ, Pachepsky Y. Fractal models for predicting soil hydraulic properties: A review. Eng Geol 1997;48(3–4):161–83.
[128] Su N, Sander GC, Liu F, Anh Vo, Barry DA. Similarity solutions for solute transport in fractal porous media using a time-and scale-dependent dispersivity. Appl Math Model 2005;29(9):852–70.
[129] Wheatcraft SW, Tyler SW. An explanation of scale-dependent dispersivity in heterogeneous aquifers using concepts of fractal geometry. Water Resour Res 1988;24(4):566–78.
[130] O'Shaughnessy B, Procaccia I. Analytical Solutions for Diffusion on Fractal Objects. Physrevlett 1985;54(5):455–8.
[131] Guarracino L, Rötting T, Carrera J. A fractal model to describe the evolution of multiphase flow properties during mineral dissolution. Adv Water Resour 2014;67:78–86.
[132] Selmi T, Seffen M, Sammouda H, Mathieu S, Jagiello J, Celzard A, et al. Physical meaning of the parameters used in fractal kinetic and generalised adsorption models of Brouers-Sotolongo. Adsorption 2018;24(1):11–27.
[133] Kanò F, Abe I, Kamaya H, Ueda I. Fractal model for adsorption on activated carbon surfaces: Langmuir and Freundlich adsorption. Surf Sci 2000;467(1-3):131–8.
[134] Sahimi M, Hashemi M. Wavelet identification of the spatial distribution of fractures. Geophys Res Lett 2001;28(4):611–4.
[135] Rasaei MR, Sahimi M. Upscaling of the geological models of large-scale porous media using multiresolution wavelet transformations. J Heat Transfer 2009;131(10):101007.
[136] Moslehi M, de Barros FPJ, Ebrahimi F, Sahimi M. Upscaling of solute transport in disordered porous media by wavelet transformations. Adv Water Resour 2016;96:180–9.
[137] Saberi AA. Recent advances in percolation theory and its applications. Phys Rep 2015;578:1–32.
[138] Hunt AG, Ghanbarian B, Skinner TE, Ewing RP. Scaling of geochemical reaction rates via advective solute transport. Chaos Interdiscip J Nonlin Sci 2015;25(7):075403. https://doi.org/10.1063/1.4913257.
[139] Sahimi M. Hydrodynamic dispersion near the percolation threshold: Scaling and probability densities. J Phys A: Math Gen 1987;20(18):L1293–8.
[140] Stauffer D. COMMENT: Monte Carlo study of biased diffusion at the percolation threshold. J Phys A: Math Gen 1985;18(10):1827–9.
[141] Stauffer D. Ising spinodal decomposition at T=O in one to five dimensions. J Phys A: Math Gen 1994;27(14):5029–32.
[142] Berkowitz B, Ewing RP. Percolation theory and network modeling applications in soil physics. Surv Geophys 1998;19(1):23–72.
[143] Guin A, Ritzi RW. Studying the effect of correlation and finite-domain size on spatial continuity of permeable sediments. Geophys Res Lett 2008;35(10).
[144] Katz AJ, Thompson AH. A Quantitative Prediction of Permeability in Porous Rock. Phys Rev B Condens Matter 1987;34(11):8179–81.
[145] Bernabé Y, Bruderer C. Effect of the variance of pore size distribution on the transport properties of heterogeneous networks. J Geophys Res Solid Earth 1998;103(B1):513–25.
[146] Katz AJ, Thompson AH. Quantitative prediction of permeability in porous rock. Phys Rev B 1986;34(11):8179–81.
[147] Nishiyama N, Yokoyama T. Estimation of permeability of sedimentary rocks by applying water-expulsion porosimetry to Katz and Thompson model. Eng Geol 2014;177:75–82.
[148] Thompson AH. Fractals in rock physics. Annu Rev Earth Planet Sci 1991;19(1):237–62.
[149] Ghanbarian B, Torres-Verdín C, Skaggs TH. Quantifying tight-gas sandstone permeability via critical path analysis. Adv Water Resour 2016;92:316–22.
[150] Skaggs TH. Assessment of critical path analyses of the relationship between permeability and electrical conductivity of pore networks. Adv Water Resour 2011;34(10):1335–42.
[151] Daigle H. Application of critical path analysis for permeability prediction in natural porous media. Adv Water Resour 2016;96:43–54.
[152] Friedman SP, Seaton NA. Critical path analysis of the relationship between permeability and electrical conductivity of three-dimensional pore networks. Water Resour Res 1998;34(7):1703–10.
[153] Hunt AG, Gee GW. Application of critical path analysis to fractal porous media: comparison with examples from the Hanford site. Adv Water Resour 2002;25(2):129–46.
[154] Hunt A, Ewing R, Ghanbarian B. Percolation theory: Topology and structure. Percolation Theory for Flow in Porous Media. Cham: Springer; 2014. p. 1–35.
[155] Sheppard AP, Knackstedt MA, Pinczewski WV, Sahimi M. Invasion percolation: new algorithms and universality classes. J Phys A: Math Gen 1999;32(49):L521–9.
[156] LeCun Y, Bengio Y, Hinton G. Deep learning. Nature 2015;521(7553):436–44.
[157] Goodfellow I, Bengio Y, Courville A. Deep learning. London: The MIT Press; 2016.
[158] Shen C, Elshorbagy A, Gupta H, Nearing G. Big Data & Machine Learning in Water Sciences: Recent Progress and Their Use in Advancing Science. Water Resour Res 2018.
[159] Cecen A, Dai H, Yabansu YC, Kalidindi SR, Song Le. Material structure-property linkages using three-dimensional convolutional neural networks. Acta Mater 2018;146:76–84.
[160] Saxena N, Mavko G, Hofmann R, Srisutthiyakorn N. Estimating permeability from thin sections without reconstruction: Digital rock study of 3D properties from 2D images. Comput Geosci 2017;102:79–99.
[161] Wu J, Yin X, Xiao H. Seeing permeability from images: fast prediction with convolutional neural networks. Science Bulletin 2018;63(18):1215–22.
[162] Wu H, Fang W-Z, Kang Q, Tao W, Qiao R. Predicting effective diffusivity of porous media from images by deep learning. Sci Rep 2019;9(1):1–12.
[163] Kamrava S, Tahmasebi P, Sahimi M. Enhancing images of shale formations by a hybrid stochastic and deep learning algorithm. Neural Networks 2019;118:310–20.
[164] Araya SN, Ghezzehei TA. Using machine learning for prediction of saturated hydraulic conductivity and its sensitivity to soil structural perturbations. Water Resour Res 2019;55(7):5715–37.
[165] Rao C, Liu Y. Three-dimensional convolutional neural network (3D-CNN) for heterogeneous material homogenization. arXiv preprint arXiv:200207600; 2020.
[166] Andrianov N, Nick HM. Machine learning of dual porosity model closures from discrete fracture simulations. Adv Water Resour 2021;147:103810. https://doi.org/10.1016/j.advwatres.2020.103810.
[167] Allaire G. Homogenization and two-scale convergence. SIAM J Math Anal 1992;23(6):1482–518.
[168] Pavliotis G, Stuart A. Multiscale methods: averaging and homogenization. Germany: Springer; 2008.
[169] da Silva EB, Souza D, de Souza AU, de Souza SGU. Prediction of effective diffusivity tensors for bulk diffusion with chemical reactions in porous media. Braz J Chem Eng 2007;24(1):47–60.
[170] Auriault J-L, Boutin C, Geindreau C. Homogenization of coupled phenomena in heterogenous media. London: John Wiley & Sons; 2010.
[171] Tartar L. H-measures, a new approach for studying homogenisation, oscillations and concentration effects in partial differential equations. Proc Roy Soc Edinb Sect A: Math 1990;115(3–4):193–230.
[172] Picchi D, Battiato I. Relative permeability scaling from pore-scale flow regimes. Water Resour Res 2019;55(4):3215–33.
[173] Amanbek Y, Singh G, Wheeler MF, van Duijn H. Adaptive numerical homogenization for upscaling single phase flow and transport. J Comput Phys 2019;387:117–33.
[174] Metzger S, Knabner P. Homogenization of two-phase flow in porous media from pore to darcy scale: A phase-field approach 2020;arXiv preprint arXiv:2002.02531.
[175] Chakib A, Hadri A, Nachaoui A, Nachaoui M. Multiscale computational method for nonlinear heat transmission problem in periodic porous media. Appl Numer Math 2020;150:164–81.
[176] Chew AWZ, Law AW-K. Homogenization theory with multiscale perturbation analysis for supervised learning of complex adsorption-desorption process in porous-media systems. J Comput Sci 2020;40.
[177] Lopes TV, Rocha AC, Murad MA, Garcia ELM, Pereira PA, Cazarin CL. A new computational model for flow in karst-carbonates containing solution-collapse breccias. Comput Geosci 2020;24(1):61–87.
[178] Mikelic A, Rosier C. Modeling solute transport through unsaturated porous media using homogenization I. Comput Appl Math 2004;23(2–3):195–211.
[179] Brenner H. Dispersion resulting from flow through spatially periodic porous media. Philosophcal Trans Roy Soc London Series A, Math Phys Sci 1980;297(1430):81–133.

[180] Aris R. On the dispersion of a solute in a fluid flowing through a tube. Process Syst Eng 1956;235(1200):67–77.
[181] Horn FJM. Calculation of dispersion coefficients by means of moments. AIChE J 1971;17(3):613–20.
[182] Wen X-H, Gómez-Hernández JJ. Upscaling hydraulic conductivities in heterogeneous media: An overview. J Hydrol 1996;183(1–2).
[183] Chrysikopoulos CV. Effective parameters for flow in saturated heterogeneous porous media. J Hydrol 1995;170(1–4):181–97.
[184] Chrysikopoulos CV, Kitanidis PK, Roberts PV. Analysis of one-dimensional solute transport through porous media with spatially variable retardation factor. Water Resour Res 1990;26(3):437–46.
[185] Chrysikopoulos CV, Kitanidis PK, Roberts PV. Macrodispersion of sorbing solutes in heterogeneous porous formations with spatially periodic retardation factor and velocity field. Water Resour Res 1992;28(6):1517–29.
[186] Dagan G. Analysis of flow through heterogeneous random aquifers. 2. Unsteady flow in confined formations. Water Resour Res 1982;18(5):1571–85.
[187] Adrover A, Passaretti C, Venditti C, Giona M. Exact moment analysis of transient dispersion properties in periodic media. Phys Fluids 2019;31(11):112002. https://doi.org/10.1063/1.5127278.
[188] Kitanidis PK. Prediction by the method of moments of transport in a heterogeneous formation. J Hydrol 1988;102(1–4):453–73.
[189] Kitanidis PK. Effective hydraulic conductivity for gradually varying flow. Water Resour Res 1990;26(6):1197–208.
[190] Shapiro M, Brenner H. Dispersion of a chemically reactive solute in a spatially periodic model of a porous medium. Chem Eng Sci 1988;43(3):551–71.
[191] Brenner H, Dorfman KD. Generalized Taylor-Aris Dispersion in Spatially Periodic Microfluidic Networks. Chemical Reactions. SIAM J Appl Math 2003;63(3):962–86.
[192] Mohamed M, Hatfield K, Perminova IV. Evaluation of monod kinetic parameters in the subsurface using moment analysis: Theory and numerical testing. Adv Water Resour 2007;30(9):2034–50.
[193] Tartakovsky AM, Panzeri M, Tartakovsky GD, Guadagnini A. Uncertainty quantification in scale-dependent models of flow in porous media. Water Resour Res 2017;53(11):9392–401.
[194] Leung JY, Srinivasan S. Effects of reservoir heterogeneity on scaling of effective mass transfer coefficient for solute transport. J Contam Hydrol 2016;192:181–93.
[195] Vikhansky A, Ginzburg I. Taylor dispersion in heterogeneous porous media: Extended method of moments, theory, and modelling with two-relaxation-times lattice Boltzmann scheme. Phys Fluids 2014;26(2):022104. https://doi.org/10.1063/1.4864631.
[196] Porta GM, Riva M, Guadagnini A. Upscaling solute transport in porous media in the presence of an irreversible bimolecular reaction. Adv Water Resour 2012;35:151–62.
[197] Dai Z, Ritzi RW, Dominic DF. Improving permeability semivariograms with transition probability models of hierarchical sedimentary architecture derived from outcrop analog studies. Water Resour Res 2005;41:W07032.
[198] Whitaker S. The method of volume averaging. New York: Springer; 1999.
[199] Aguilar-Madera CG, Herrera-Hernández EC, Espinosa-Paredes G. Solute transport in heterogeneous reservoirs: Upscaling from the Darcy to the reservoir scale. Adv Water Resour 2019;124:9–28.
[200] Yang C, Huang R, Lin Y, Qiu T. Volume averaging theory (VAT) based modeling for longitudinal mass dispersion in structured porous medium with porous particles. Chem Eng Res Des 2020;153:582–91.
[201] Orgogozo L, Golfier F, Buès MA, Quintard M, Koné T. A dual-porosity theory for solute transport in biofilm-coated porous media. Adv Water Resour 2013;62:266–79.
[202] Aguilar-Madera CG, Herrera-Hernández EC, Espinosa-Paredes G. Effective equation to assess solute transport in two-lithology reservoirs. J Hydrol 2020;124648.
[203] Quintard M, Whitaker S. Convection, dispersion, and interfacial transport of contaminants: Homogeneous porous media. Adv Water Resour 1994;17(4):221–39.
[204] Wood BD, Cherblanc F, Quintard M, Whitaker S. Volume averaging for determining the effective dispersion tensor: Closure using periodic unit cells and comparison with ensemble averaging. Water Resour Res 2003;39(8):1210.
[205] Qiu T, Wang Q, Yang C. Upscaling multicomponent transport in porous media with a linear reversible heterogeneous reaction. Chem Eng Sci 2017;171:100–16.
[206] Dai Z, Keating E, Gable C, Levitt D, Heikoop J, Simmons A. Stepwise inversion of a groundwater flow model with multi-scale observation data. Hydrogeol J 2010;18(3):607–24.
[207] Dai Z, Zhan C, Dong S, Yin S, Zhang X, Soltanian MR. How does resolution of sedimentary architecture data affect plume dispersion in multiscale and hierarchical systems? J Hydrol 2020;582:124516.
[208] Gelhar LW, Axness CL. Three-dimensional stochastic analysis of macrodispersion in aquifers. Water Resour Res 1983;19(1):161–80.
[209] Durst F, Miloievic D, Schönung B. Eulerian and Lagrangian predictions of particulate two-phase flows: a numerical study. Appl Math Model 1984;8(2):101–15.
[210] Gelhar LW, Axness CL. Reply [to "Comment On 'Three-dimensional stochastic analysis of macrodispersion in aquifers' by Lynn W. Gelhar and Carl L. Axness"]. Water Resour Res 1983;19(6):1643–4.
[211] Liao Q, Lei G, Zhang D, Patil S. Analytical solution for upscaling hydraulic conductivity in anisotropic heterogeneous formations. Adv Water Resour 2019;128:97–116.
[212] Nachabe MH, Morel-Seytoux HJ. Perturbation and Gaussian methods for stochastic flow problems. Adv Water Resour 1995;18(1):1–8.
[213] Berkowitz B. Dispersion in heterogeneous geological formations. Springer; 2001.
[214] Morales-Casique E, Neuman SP, Guadagnini A. Non-local and localized analyses of non-reactive solute transport in bounded randomly heterogeneous porous media: Theoretical framework. Adv Water Resour 2006;29(8):1238–55.
[215] Liou T-S, Yeh H-D. Conditional expectation for evaluation of risk groundwater flow and solute transport: one-dimensional analysis. J Hydrol 1997;199(3–4):378–402.
[216] Li S-G, McLaughlin D, Liao H. The accuracy of stochastic perturbation solutions to subsurface transport problems. Adv Water Resour 2004;27(1):47–56.
[217] Ginting V, Ewing R, Efendiev Y, Lazarov R. Upscaled modeling in multiphase flow applications. Comput Appl Math 2004;23(2–3):213–33.
[218] Soltanian MR, Behzadi F, de Barros FPJ. Dilution enhancement in hierarchical and multiscale heterogeneous sediments. J Hydrol 2020;587.
[219] Rubin Y. Flow and transport in bimodal heterogeneous formations. Water Resour Res 1995;31(10):2461–8.
[220] Lu Z, Zhang D. On stochastic study of well capture zones in bounded, randomly heterogeneous media. Water Resour Res 2003;39(4):1100.
[221] Dai Z, Ritzi Jr RW, Huang C, Rubin YN, Dominic DF. Transport in heterogeneous sediments with multimodal conductivity and hierarchical organization across scales. J Hydrol 2004;294(1–3):66–86.
[222] Dentz Marco, Cortis Andrea, Scher Harvey, Berkowitz Brian. Time behavior of solute transport in heterogeneous media: transition from anomalous to normal transport. Adv Water Resour 2004;27(2):155–73.
[223] Ritzi RW, Dai Z, Dominic DF, Rubin YN. Spatial correlation of permeability in cross-stratified sediment with hierarchical architecture. Water Resour Res 2004;40(3).
[224] Huang Chaocheng, Dai Zhenxue. Modeling groundwater in multimodal porous media with localized decompositions. Math Geosci 2008;40(6):689–704.
[225] Ritzi RW, Dai Z, Dominic DF, Rubin YN. Spatial correlation of permeability in cross-stratified sediment with hierarchical architecture. Water Resour Res 2004;40:W03513.
[226] Soltanian Mohamad Reza, Ritzi Robert, Dai Zhenxue, Huang Chaocheng, Dominic David. Transport of kinetically sorbing solutes in heterogeneous sediments with multimodal conductivity and hierarchical organization across scales. Stoch Env Res Risk Assess 2015;29(3):709–26.
[227] Dai Z, Wolfsberg A, Lu Z, Deng H. Scale dependence of sorption coefficients for contaminant transport in saturated fractured rock. Geophys Res Lett 2009;36(1).
[228] Bellin Alberto, Rinaldo Andrea, Bosma Willem Jan P, van der Zee Sjoerd EATM, Rubin Yoram. Linear equilibrium adsorbing solute transport in physically and chemically heterogeneous porous formations: 1. Analytical solutions. Water Resour Res 1993;29(12):4019–30.
[229] Rajaram Harihar. Time and scale dependent effective retardation factors in heterogeneous aquifers. Adv Water Resour 1997;20(4):217–30.
[230] Cvetkovic Vladimir, Fiori Aldo, Dagan Gedeon. Solute transport in aquifers of arbitrary variability : A time-domain random walk formulation. Water Resour Res 2014;50(7):5759–73.
[231] Barrash Warren, Clemo Tom. Hierarchical geostatistics and multifacies systems: Boise Hydrogeophysical Research Site, Boise, Idaho. Water Resour Res 2002;38(10):14-1–14-18.
[232] Deng Hailin, Dai Zhenxue, Wolfsberg Andrew V, Ye Ming, Stauffer Philip H, Lu Zhiming, et al. Upscaling retardation factor in hierarchical porous media with multimodal reactive mineral facies. Chemosphere 2013;91(3):248–57.
[233] Soltanian Mohamad Reza, Ritzi Robert W, Dai Zhenxue, Huang Chao Cheng. Reactive solute transport in physically and chemically heterogeneous porous media with multimodal reactive mineral facies: The Lagrangian approach. Chemosphere 2015;122:235–44.
[234] Soltanian Mohamad Reza, Sun Alexander, Dai Zhenxue. Reactive transport in the complex heterogeneous alluvial aquifer of Fortymile Wash, Nevada. Chemosphere 2017;179:379–86.
[235] Dean DW, Russell TF. A numerical Lagrangian stochastic approach to upscaling of dispersivity in solute transport. Adv Water Resour 2004;27(4):445–64.
[236] Paster Amir, Bolster Diogo, Benson David A. Connecting the dots: Semi-analytical and random walk numerical solutions of the diffusion–reaction equation with stochastic initial conditions. J Comput Phys 2014;263:91–112.
[237] Ding Dong, Benson David A, Fernàndez-Garcia Daniel, Henri Christopher V, Hyndman David W, Phanikumar Mantha S, et al. Elimination of the reaction rate "scale effect": Application of the lagrangian reactive particle-tracking method to simulate mixing-limited, field-scale biodegradation at the Schoolcraft (MI, USA) site. Water Resour Res 2017;53(12):10411–32.
[238] Rubin Yoram, Chang Ching-Fu, Chen Jiancong, Cucchi Karina, Harken Bradley, Heße Falk, et al. Stochastic hydrogeology's biggest hurdles analyzed and its big blind spot. Hydrol Earth Syst Sci 2018;22(11):5675–95.
[239] Rajaram H. Debates—Stochastic subsurface hydrology from theory to practice: Introduction. Wiley Online. Library 2016.
[240] Straubhaar J. DeeSse user's guide. Neuchâtel, Switzerland: The Centre for Hydrogeology and Geothermics (CHYN), University of Neuchâtel; 2019.
[241] Remy N, Boucher A, Wu J. Applied geostatistics with SGeMS: A user's guide. Cambridge University Press; 2009.
[242] Park Moongyu, Cushman John H. On upscaling operator-stable Lévy motions in fractal porous media. J Comput Phys 2006;217(1):159–65.
[243] O'Malley D, Cushman JH, Johnson G. Scaling laws for fractional Brownian motion with power-law clock. J Stat Mech: Theory Exp 2011;2011(01):L01001.
[244] Metzler Ralf, Jeon Jae-Hyung, Cherstvy Andrey G, Barkai Eli. Anomalous diffusion models and their properties: Non-stationarity, non-ergodicity, and ageing at the centenary of single particle tracking. PCCP 2014;16(44):24128–64.

[245] Molz FJ, Liu HH, Szulga J. Fractional brownian motion and fractional gaussian noise in subsurface hydrology: A review, presentation of fundamental properties, and extensions. Water Resour Res 1997;33(10):2273–86.
[246] Liu HH, Molz FJ. Multifractal analyses of hydraulic conductivity distributions. Water Resour Res 1997;33(11):2483–8.
[247] Herrera-Hernández EC, Aguilar-Madera CG, Ocampo-Perez R, Espinosa-Paredes G, Núñez-López M. Fractal continuum model for the adsorption-diffusion process. Chem Eng Sci 2019;197:98–108.
[248] Zhokh Alexey, Strizhak Peter. Investigation of the anomalous diffusion in the porous media: a spatiotemporal scaling. Heat Mass Transf 2019;55(9):2693–702.
[249] Ndumu Alberto S, Addison Paul S. Scale-dependent subsurface dispersion: A fractal-based stochastic model. J Hydrol Eng 2001;6(1):34–42.
[250] Agboola O, Onyango MS, Popoola P, Oyewo OA. Fractal geometry and porosity. Fractal Analysis-Applications in Physics. Eng Technol 2017.
[251] Navarre-Sitchler A, Brantley S. Basalt weathering across scales. Earth Planet Sci Lett 2007;261(1–2):321–34.
[252] Nikan O, Machado JA Tenreiro, Golbabai A, Nikazad T. Numerical approach for modeling fractal mobile/immobile transport model in porous and fractured media. Int Commun Heat Mass Transfer 2020;111:104443. https://doi.org/10.1016/j.icheatmasstransfer.2019.104443.
[253] Ritzi RW, Soltanian MR. What have we learned from deterministic geostatistics at highly resolved field sites, as relevant to mass transport processes in sedimentary aquifers? J Hydrol 2015;531:31–9.
[254] Dai Z, Ritzi Jr RW, Dominic DF. Improving permeability semivariograms with transition probability models of hierarchical sedimentary architecture derived from outcrop analog studies. Water Resour Res 2005;41(7).
[255] Ritzi RW, Huang L, Ramanathan R, Allen-King RM. Horizontal spatial correlation of hydraulic and reactive transport parameters as related to hierarchical sedimentary architecture at the Borden research site. Water Resour Res 2013;49(4):1901–13.
[256] Sarfaraz SM, Rosić BV, Matthies HG, Ibrahimbegović A. Stochastic upscaling via linear Bayesian updating Multiscale. In: Modeling of Heterogeneous Structures. Springer; 2018. p. 163–81.
[257] Ye M, Neuman SP, Meyer PD. Maximum likelihood Bayesian averaging of spatial variability models in unsaturated fractured tuff. Water Resour Res 2004;40:W05113.
[258] Cirpka OA, Valocchi AJ. Debates—Stochastic subsurface hydrology from theory to practice: Does stochastic subsurface hydrology help solving practical problems of contaminant hydrogeology? Water Resour Res 2016;52(12):9218–27.
[259] Liu G, Zhang D, Lu Z. Stochastic uncertainty analysis for unconfined flow systems. Water Resour Res 2006;42(9).